



Structure and Infrastructure Engineering

Maintenance, Management, Life-Cycle Design and Performance

ISSN: (Print) (Online) Journal homepage: <https://www.tandfonline.com/loi/nsie20>

Seismic risk prioritisation schemes for reinforced concrete bridge portfolios

Andres Abarca, Ricardo Monteiro & Gerard J. O'Reilly

To cite this article: Andres Abarca, Ricardo Monteiro & Gerard J. O'Reilly (2023): Seismic risk prioritisation schemes for reinforced concrete bridge portfolios, Structure and Infrastructure Engineering, DOI: [10.1080/15732479.2023.2187424](https://doi.org/10.1080/15732479.2023.2187424)

To link to this article: <https://doi.org/10.1080/15732479.2023.2187424>



Published online: 07 Mar 2023.



Submit your article to this journal [↗](#)



View related articles [↗](#)



View Crossmark data [↗](#)



Seismic risk prioritisation schemes for reinforced concrete bridge portfolios

Andres Abarca , Ricardo Monteiro  and Gerard J. O'Reilly 

University School for Advanced Studies (IUSS) of Pavia, Pavia, Italy

ABSTRACT

A significant portion of the existing bridge inventory in Italy is decades old, requiring continuous maintenance and safety assessment approaches. Recent collapses of existing reinforced concrete bridges have piqued public interest, placing pressure on management agencies to define methodologies with which to prioritise asset maintenance and to effectively utilise their limited resources. When looking for decision variables to perform this prioritisation, seismic risk assessment metrics, such as average annual losses (AAL), are an appealing choice. However, obtaining this metric for a large bridge inventory is technically challenging and requires large amounts of information that are seldom available, promoting the development of practical approaches that can predict the relative priority of assets within a portfolio, based on processing simple indicators with acceptable accuracy. In this research, a case study of 617 bridges from the Italian road network was assessed considering state-of-the-art approaches to calculate total losses. The results were explored with data science techniques, identifying the main features that drive the relative importance of bridges in terms of AAL and using them as guidance to calibrate a simplified methodology, based on the recent Italian Guidelines for Bridge Safety Assessment. The proposed AAL-based modifications demonstrate a notable improvement in the definition of bridge assessment priorities, as well as providing further resolution in the classification for more efficient decision making.

ARTICLE HISTORY

Received 30 November 2021
Revised 19 October 2022
Accepted 8 December 2022

KEYWORDS

Bridges; machine learning; prioritization; regional seismic risk; road networks; transportation infrastructure

1. Introduction

Bridges form an integral part of road networks and provide crucial access between regions and cities, however, their presence has become so normalised in modern times that their existence and importance can go unnoticed to the regular user. The bridge inventory of developed countries can reach thousands of assets that have been built over several decades by different administrations (Calvi et al., 2019), creating a challenge for the institutions currently managing these large portfolios of bridges for which there is incomplete information about their current structural condition and limited resources available to upgrade or maintain them.

In the case of Italy, a great portion of its current infrastructure was built during a construction surge of freeways that happened all over Europe in the 1960s (Calvi et al., 2019). This coincided with a period in which the design codes of bridges referred to much lighter vehicular loads than the ones recommended for current traffic loading (Iatsko & Nowak, 2021) and the consideration of extreme demands from natural events, such as earthquakes, was still in development. Furthermore, the longevity of the current inventory, aided by the difficulties of management agencies in providing proper maintenance, has led to a generalised problem of deterioration that increases the vulnerability of

these structures, a condition that has become evident by the number of bridge collapses in recent years.

Recent notable cases in Italy have attracted media attention to this problem, such as the collapse of the Morandi Bridge (Viadotto Polcevera) in Genova in August 2018, but many other collapses have happened in Italy with a non-negligible effect on the road system. For example, a non-exhaustive list of collapses collected from reports in the media is presented in Table 1, where it can be observed that several months or even years can pass for a bridge to be reopened following its full or partial collapse. This considerably interrupts the network for an extended period, also impacting the local and wider community due to the loss of a potentially key element of the overall infrastructure system.

Considering the situation described above, there is a real need for bridge management institutions to determine rapid prioritisation methods that, based on the limited information available about assets in the inventory, allow the identification of the assets requiring special attention in the form of inspection, detailed analysis, monitoring and possible retrofitting. Such prioritisation methodologies have been the source of multiple research efforts worldwide. A summary is available in a recent technical report by the United States Department of Transportation (Chase, Adu-Gyamfi, Aktan, & Minaie, 2016). It documents the evolution and application of different bridge health indices used by bridge

Table 1. Bridge collapses reported in Italy since 2004.

#	Region	Province	Bridge Name/Location	Length (m)	Collapse Date	Re-opening Date
1	Friuli Venezia Giulia	Pordenone	Viadotto del Chiavalir	25.00	Dec-04	Jul-09
2	Liguria	Genova	Carasco	258.00	Oct-13	Apr-14
3	Sardinia	Nuoro	Oliena-Dorgali	130.00	Nov-13	Jan-20
4	Sicily	Agrigento	Lauricella-Petrulla	476.00	Jul-14	Mar-18
5	Lombardy	Lecco	Annone	56.00	Oct-16	Jul-19
6	Marche	Ancona	Ancona	45.00	Mar-17	Jun-18
7	Liguria	Genova	Viadotto Polcevera	1182.00	Aug-18	Aug-20
8	Liguria	Savona	Madonna del Monte	30.00	Nov-19	Feb-20
9	Toscana	Massa-Carrara	Albiano Magra	290.00	Apr-20	Mar-22
10	Piedmont	Novara	Romagnano Sesia	156.00	Oct-20	Aug-21

management agencies interested in preserving the condition of bridge structures or prioritising the maintenance or replacement projects within their bridge inventory.

Mostly, these methodologies rely on element-level information of each bridge to assess its current state and service level; however, they typically do not include aspects of resilience and the importance of each asset on the overall network that they form a part of. An example of such a methodology that is regularly used in the United States, Canada, Italy and Japan employs the Bridge Health Index or Bridge Condition Index (Shepard & Johnson, 2001), given by the ratio between the current condition of a bridge and the one expected right after construction, measured in terms of a weighted average of element-based indexes that record deterioration from inspection information, thus providing information on the current residual state of an asset compared to a pristine structure.

Other recent examples include the Bridge Overall Priority Indicator (Mohamed et al., 2019), developed for the Egyptian context, and the Bridge Priority Index (Rashidi et al., 2015), for the Australian context; both of which use an empirical approach based on expert opinion to identify key indicators of expected performance through inspection data. Other sources can be classified as risk-based approaches, such as the Integrated Bridge Index (Valenzuela, De Solminihac, & Echaveguren, 2009), developed for the Chilean context, which weighs factors such as seismic risk, hydraulic vulnerability and strategic importance to aid in prioritization and rehabilitation of bridges in a portfolio.

Recent Italian examples include the simplified index-based methods developed by Pellegrino, Pipinato, and Modena (2011) and D'Apuzzo et al. (2019), which are both based on detailed inspection-level information to assess the deterioration status of the bridges and combine it with the importance of each asset to the overall network by incorporating an additional index based on road typology and traffic flows. More recently, the Italian Superior Council of Public Works, within the Ministry of Infrastructure and Transport (MIT), issued a technical report with guidelines on risk classification and management, safety assessment and the monitoring of existing bridges (Consiglio Superiore dei Lavori Pubblici, 2020), which has already become part of the mandatory legislation for bridge management institutions and concessionaries in Italy (Ministero delle Infrastrutture e dei Trasporti, 2020). This document, which will be referred to from this point forward as the 2020 MIT Guidelines, intends to standardise the procedure with which

existing bridges in Italy are assessed at a large scale by a multi-level and multi-component approach that classifies bridges in risk categories via a combination of qualitative metrics.

Among most of the sources that deal with the prioritisation of bridges in a portfolio, there are similarities about the components that should be ideally included when determining the relative importance of assets and their urgency in attention:

- Accounting for the demands deriving from multiple hazards such as: traffic loads, flooding, earthquakes and landslides.
- The overall properties of the assets, such as: structural typology, dimensions, mechanical properties, cost of the infrastructure and its relative importance to the operation of the road network.
- State of degradation, corrosion and overall expected performance of the bridge components when subjected to the considered hazards.

While these components are generally included in the available proposals for simplified prioritisation in different ways, there is a difficulty in assessing their relative importance and, therefore, the way in which they are processed is typically defined by expert opinion. When looking for an established metric that allows the consideration of the entire scope of the problem in a single value, average annual loss (AAL) is a risk metric that has seen growing use within the structural engineering community (O'Reilly & Calvi, 2019; Shahnazaryan & O'Reilly, 2021), even being proposed as a target metric to be used in new methods for structural design and assessment (Calvi, O'Reilly, & Andreotti, 2021). AAL, also referred to in some sources as expected annual loss (EAL), is a product of risk assessment that represents long-term expected economic losses per year, averaged over many years, that are produced by specific hazards of varying intensities and their respective annual exceedance rates, or return periods.

In this paper, a seismic risk methodology is applied to a case study of 617 bridges in the Italian province of Salerno to determine prioritisation of assets based on AAL, which is then used for two main purposes: as a benchmark to compare with the results obtained using the recent 2020 MIT Guidelines and as a possible guiding parameter to determine the relative importance of each factor affecting the determination of priority, with a view to moving towards a more optimised but still simple prioritisation approach.

2. Methodology

The methodology defined for this study, depicted graphically in Figure 1, initially consisted of creating a synthetic case study, given by a portfolio of bridges with fully known information located within an existing road network. This case study was then used to apply detailed risk assessment procedures, leading to the calculation of the AAL for each asset, thus creating a benchmark with which to evaluate different prioritisation methodologies and the influence of multiple parameters on the overall performance of the inventory. A database containing 308 bridges from the National Autonomous Roads Corporation ANAS (*Azienda Nazionale Autonoma delle Strade*) inventory (Borzi et al., 2015), collected and managed by the Eucentre Foundation, was used to populate a model of the primary and secondary road network of the Italian province of Salerno. The model was built from information taken from OpenStreetMap repositories (OpenStreetMap contributors, 2020), such as connectivity, number of lanes, road typology and traffic flow capacity.

Once the case study was defined, a probabilistic seismic hazard analysis was carried out for the location of each bridge to determine hazard curves specific to each site. Furthermore, all bridges were grouped into four hazard zones, where a conditional spectrum record selection was carried out considering two possible soil conditions (soft and stiff) to obtain ground motion record sets for each zone. These sets of 30 bi-directional earthquake records were conditioned on average spectral acceleration, AvgSa, which is an intensity measure recently shown to be quite advantageous when assessing multiple bridge structures (Abarca, Monteiro, O'Reilly, Zuccolo, & Borzi, 2023) when compared to more common intensity measures adopted in previous studies in the field. AvgSa was defined for the

period range of 0.1s to 1.7s considering a spacing of 0.1s and was used to condition the record selection for nine return periods of ground shaking, ranging from 98 to 9975 years.

Numerical models were created for each bridge using the BRITNEY modelling tool, developed by Borzi et al. (2015) and were analysed using the ground motion record set corresponding to the location of each asset to perform non-linear time-history analysis (NLTHA). The NLTHA results were then processed to determine fragility curves for the collapse limit state of each case-study bridge in terms of AvgSa, which differs from the original BRITNEY framework that employed peak ground acceleration (PGA) as intensity measure. These fragility curves were integrated with the hazard curves of each site to obtain the annual probability of collapse of each bridge.

To obtain a complete account of the AALs that can be attributed to the collapse of each bridge due to seismic hazard, both the direct replacement cost as well as the indirect cost of the bridge should be considered. While the direct cost can be taken as proportional to the deck area multiplied by an average construction cost value, the indirect counterpart requires an analysis of the transportation network to evaluate the economic loss that the users would incur because of the disruption caused by the collapse of each bridge. Once the total (direct and indirect) replacement costs of each asset were calculated, they were combined with the annual probability of collapse to determine an expected AAL for each bridge, defining an AAL database that can be used as a benchmark prioritisation metric.

This database was then explored through data science methodologies, including a machine learning model, to gain insights on how some of the simple features (e.g. span length, structural typology, pier height, etc.) that are commonly available for each bridge can be used as indicators to

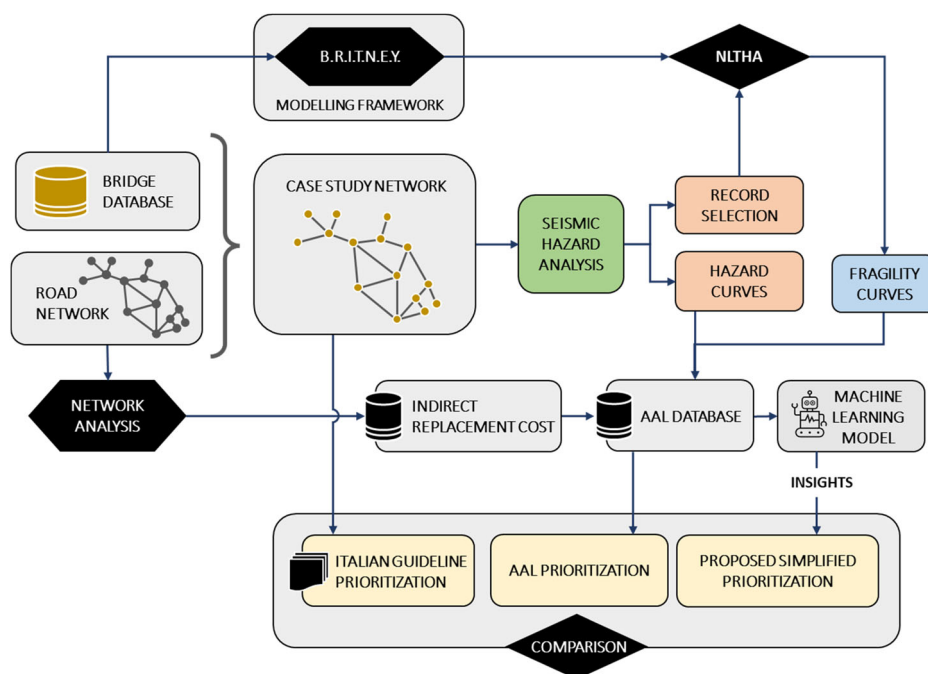


Figure 1. Methodology used to understand the implementation of the recent 2020 MIT Guidelines and explore improvement options.

approximate the AAL-based priority. Finally, a comparison was made between the 2020 MIT Guidelines classification, the AAL-based prioritisation and the insights obtained from the database and the machine learning model, in order to evaluate the 2020 MIT Guidelines and develop a more optimised proposal with the same level of simplicity of implementation but with improved overall accuracy, when compared with the AAL ranking.

3. Case study bridge inventory

3.1. Database description

As mentioned previously, a bridge database comprising 308 bridges from the National Autonomous Roads Corporation ANAS (*Azienda Nazionale Autonoma delle Strade*) inventory, collected and managed by the Eucentre Foundation, was considered to create the case study for this research. These bridges form a part of the Italian road network, and their actual geographic location is scattered along the primary highway grid of Italy, as shown in Figure 2.

The information available in the database represents a complete ‘as-built’ account of geometrical and structural properties of the bridges, without consideration of observed damage or deterioration, allowing detailed structural numerical models of each asset to be created. Each asset in the database is a reinforced concrete (RC) bridge with two or more spans, a predominant configuration in the Italian road network (Zelaschi et al., 2016). In terms of general dimensions, the overall number of spans ranges from 2 to 36, which translates to an overall bridge length range of 50 m to 1250 m. A large portion of the inventory is not straight, as 35% of the assets have curved decks on at least one of the spans, which sometimes makes it difficult to use the typical definition of longitudinal/transverse directions. The height



Figure 2. Location of the 308 case-study assets in the ANAS bridge inventory.

of piers ranges between 5 m and 45 m in the overall inventory and it is typical to observe large variation of the pier height within the same asset, leading sometimes to irregular dynamic configurations within straight bridges. A more complete description of the distributions of these bridge properties is shown in Figure 3. In terms of static configuration, the vast majority of the case-study assets have spans that are simply supported upon the piers with thin elastomeric pads, and only a small percentage has continuous deck and bearings that can be either elastomeric or isolators.

In terms of pier sections, the inventory includes multiple configurations, which sometimes change even within the same asset. To provide some aggregated information regarding the pier types of the inventory, three main pier types were identified: single column (SC), wall (W) and multiple column (MW) configurations, the distribution of which is shown in Figure 4(a). It is important to note that the actual pier cross sections might be composed of circular sections, box sections, elliptical or many other kinds of geometrical configurations. Nevertheless, the fragility analysis of each asset was carried out on an element-by-element basis (i.e. each bridge was specifically analysed with its respective pier properties) thus this pier type illustration had no impact on the fragility curve results.

The construction year was available for all assets, ranging between 1953 and 2000, with most of them built during the 1960s and 1970s, as shown in Figure 4(d). Information on the current state of deterioration of the assets was not available in the database. As is common for regular Italian bridges of those decades, none of them are expected to have been specifically designed to meet appropriate seismic requirements, especially considering that the first national seismic regulation in Italy that addressed the entire national territory was instated in 2003 (Consiglio dei Ministri, 2003).

In general, the reinforcement percentages in the piers, both in longitudinal (A_{sl}/A_c) and transverse (A_{st}/A_c) directions, are low in comparison to current design standards and are quite similar across the different pier sections. This is atypical under current design practices, however, both the reinforcement ratios and the properties of the materials used for construction are in line with the age of construction of the inventory. Distributions for the mechanical properties of the materials are shown in Figure 4(e) and (f). In terms of dynamic properties, a structural model was created for each asset to determine the modal periods in both orthogonal horizontal directions. Since, for the case of bridges, the first mode does not typically account for a significant percentage of the total modal mass, an appropriate number of modes were evaluated for each asset to include 85% of the modal mass in each direction. The distributions for the first modal period (T_1) and the modal period at which 85% of the modal mass is obtained ($T_{85\%}$) as shown in Figure 5.

The intensity measure chosen to perform hazard and fragility calculations was average spectral acceleration (AvgSa), for which the collective results of T_1 and $T_{85\%}$ were used to define the period range. As shown in Figure 5, the selected range was 0.1 seconds to 1.7 seconds, which was defined as per O'Reilly (2021) as 1.5 times the 84th percentile to account for period

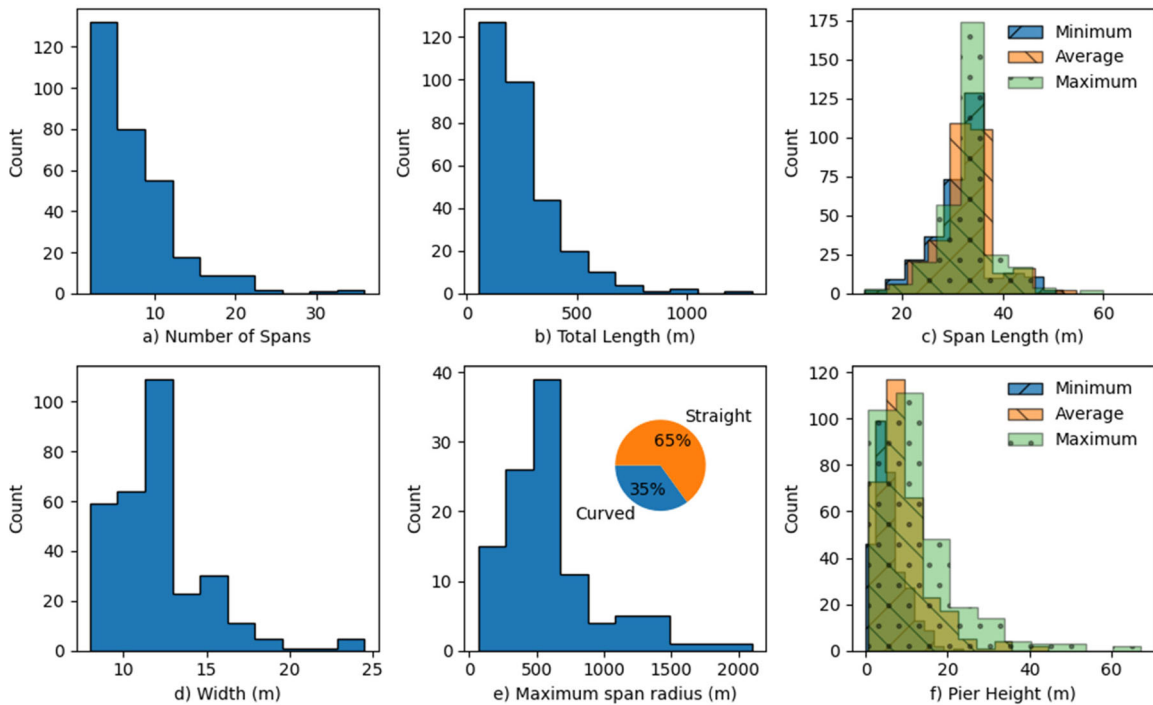


Figure 3. Distribution of general and geometrical properties of the bridge database.

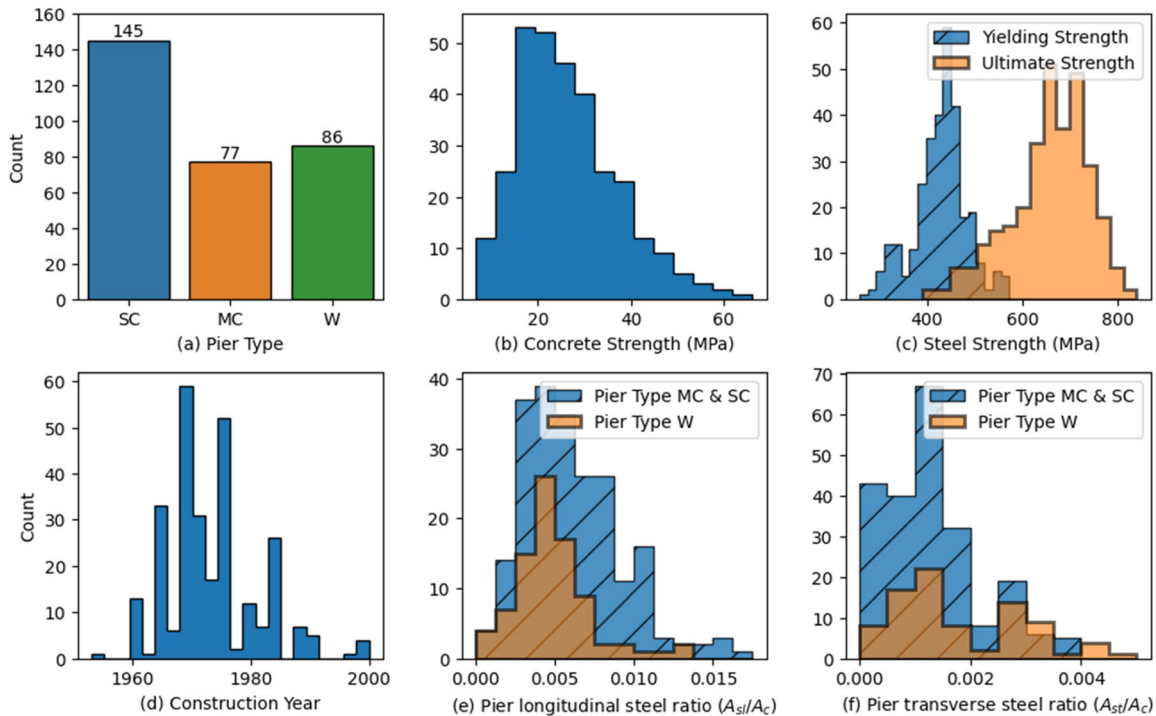


Figure 4. Distribution of main material properties of the bridge database (SC: Single Column, MC: Multiple Columns, W: Wall, Asl: Area of longitudinal steel, Ast: Area of transverse steel, Ac: gross area of the element).

elongation of the first mode and 0.5 times the 16th percentile to account for higher mode contributions of the T_1 and $T_{85\%}$ periods, respectively, for the entire inventory.

3.2. Case study description

As shown in Figure 2, the bridges in the ANAS database are scattered geographically all over the Italian territory and not

directly connected, therefore, their real location is not ideal to define a case study, since the consideration of the collective and individual role of each asset in the road network would be an unfeasible exercise. Ideally, if a case study of bridges closely connected within the same territory were available, it could be explored and fully analysed to represent a benchmark with which to evaluate the performance of simplified prioritisation frameworks. For this reason, a

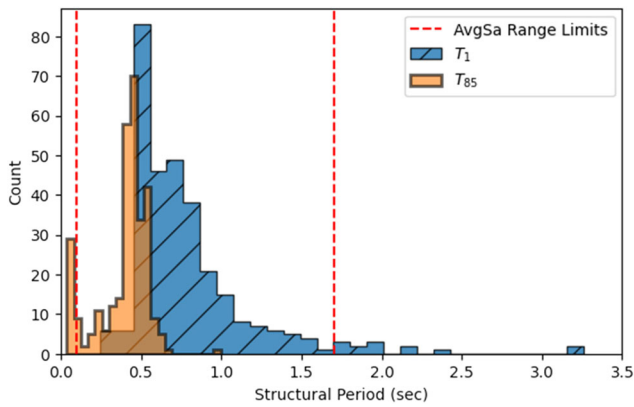


Figure 5. Results for modal structural periods of the entire inventory and definition of AvgSa range.

synthetic case study was created by taking the road network of a region for which the location of bridges and road properties was known and assigning a bridge from the 308-asset database to each location using a simple random sampling scheme.

Note that this example does not correspond to the exact real case study, in which the actual exposure inventory would include bridges with more typologies and construction materials than the ones incorporated herein (only RC bridges), even if the included typologies do represent an important percentage of the Italian bridge inventory (Borzi et al., 2015; Zelaschi et al., 2016). Furthermore, the limitation of randomly placing the bridges in locations other than the real ones, is minimised by the fact that, even when placed in locations with different seismic hazard demands, bridge design practices are not expected to have varied considerably among the Italian territory for the construction period of the bridges in the database (Borzi et al., 2015). This is also reinforced by the aforementioned fact that the first national seismic regulation in Italy that addressed the entire national territory was instated in 2003 (Consiglio dei Ministri, 2003), thus it is likely that bridges prior to this year were not highly conditioned, design wise, by the seismic hazard of the location where they were built. The sole purpose of the case study created herein is to present and evaluate the prioritization methodology hence to consider the results from this synthetic case study as a benchmark should not influence that objective.

The Salerno province was selected for having a transportation network that relies heavily on the vehicular road system and a varying seismicity level. Information about the road network of Salerno was taken from the OpenStreetMap database (OpenStreetMap contributors, 2020), which comprises all roads within the highway, primary and secondary systems, including 2929 nodes and 3086 links, of which 617 represent bridges. The centroid locations of the 158 municipalities in the Salerno province were used as traffic attraction zones (centroids) from which all trips were assumed to occur to and from. The 308 bridges in the database were therefore randomly assigned to the 617 possible locations of bridges in the Salerno network using a sampling with replacement scheme. Once the final distribution of assets in the case study was defined, a transportation network model

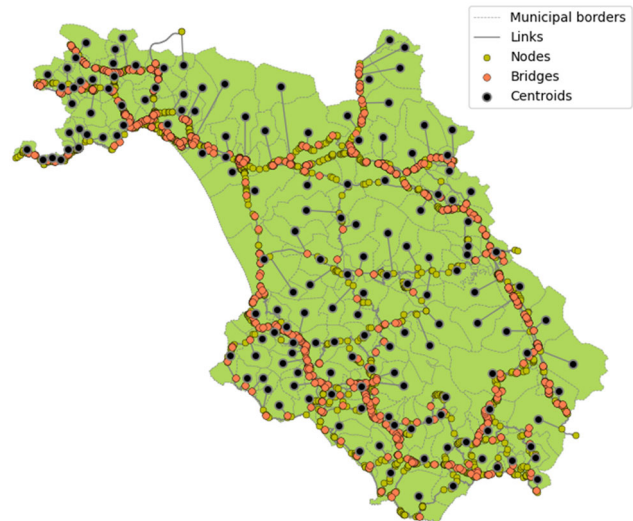


Figure 6. Road network model for the case study region of Salerno built on AequilibraE (www.aequilibrae.com) based on OpenStreetMap data.

was created using the software AequilibraE (www.aequilibrae.com), an open-source Python and QGIS package to perform transportation network analysis, to determine the baseline traffic conditions that are fundamental to assess the importance of each bridge in the network. A graphical representation of the network model is shown in Figure 6.

A database containing travel pattern information for work and study purposes performed in 2011 was taken from the Italian Institute of Statistics (ISTAT, 2014) and used to define origin-destination demands between the different municipalities of Salerno. For the sake of simplicity and to due to the need to delimitate the area of analysis, trips coming and going outside of the borders of the case study region are excluded from the analysis, which however will impact the traffic assignment. Future improvements of the framework may address this issue in a practical, feasible manner. For the current exercise, only trips performed by private car owners were considered since no information of freight or public transportation was available. It is important to note that the lack of information of trips performed by freight and public transportation vehicles constitutes a limitation of the current study, as those will have an important contribution to the calculation of the indirect losses. While this does not represent a conceptual aspect of the methodology (i.e. its formulation would not change), such information should thus definitely be included in future research and in real case studies.

In order to account for congestion in the network, previous research regarding Italian road characteristics (Maratini, 2008) was used to obtain the volume-delay function modelling parameters according to the commonly used BPR model (Bureau of Public Roads, 1964) for the different road types in the network, as shown in Table 2. Free flow speed was taken as the speed limit reported for each road in the OpenStreetMap database; while some studies (Zilske, Neumann, & Nagel, 2011) modify the speed limit values to accurately represent the free flow speed according to the case study characteristics, this was not done in this study since no precedent was found for the case study region and

Table 2. Volume-delay function parameters used for road network modelling.

Typology	Capacity (vehicles/hour/lane)	BPR parameters	
		α	β
Highway	1600	0.28	0.93
Primary	1400	0.25	1.13
Secondary	1400	0.25	1.13

the implementation of the speed limit provided good results during the validation stage, as will be demonstrated shortly.

A trip distribution based on the minimisation of travel time of each user was carried out using a bi-conjugate Frank-Wolfe algorithm (Mitradjeva & Lindberg, 2013) to determine the baseline traffic conditions of the fully operational road network. The results in terms of trip duration were compared with the corresponding values reported in the census data to validate the model. As can be seen in Figure 7, even though the model tended to predict longer travelling times in comparison to the census data, there is quite a good agreement for most of the trips overall. The mismatch for longer travel times was expected since the model does not include the entirety of roads in the network (i.e. it excludes the local residential system). As such, increased levels of congestion can occur artificially in the model by having to distribute all of the traffic demands in a reduced number of roads.

4. Seismic risk analysis

4.1. Seismic hazard and record selection

The Salerno province, as previously described, was selected as the case study region partly because it has a varied seismic hazard that ranges from low seismicity regions near the coastline, to high seismicity areas near the Southern Apennines Mountain range, which was the location of the M_w 6.9 Irpinia earthquake in 1980, for example. This wide range of seismicity represents an opportunity for this case study, as it allows possible differences in the response of bridges in different seismic demand areas to be investigated. In terms of hazard curves, the SHARE hazard model (Woessner et al., 2015), implemented in the OpenQuake Engine (Silva, Crowley, Pagani, Monelli, & Pinho, 2014), was used to determine the probability of exceedance of different levels of AvgSa for an investigation period of 50 years at each bridge site. In terms of ground motion record selection, a conditional spectrum scheme (Lin, Haselton, & Baker, 2013) was adopted using a modification that allows the conditioning of the spectra for AvgSa (Kohrangi, Bazzurro, Vamvatsikos, & Spillatura, 2017). The implementation of the record selection methodology used requires results from a disaggregation analysis to determine the mean magnitude and distance that principally drive the seismic demands at each specific site.

However, given the large number of bridge locations, and to minimise the computational burden of performing disaggregation at each location, all assets were assigned to four hazard zones and two soil classes (i.e. soft and stiff soil differentiated by a $V_{s,30}$ threshold of 360 m/s) as illustrated in

Figure 8. Following this, a complete hazard disaggregation analysis was carried out for the eight possible zone-soil combinations. For each combination, sets of 30 bidirectional ground motion records were selected from the NGA West-2 Strong-motion Database (Ancheta, et al., 2014) for nine return periods ranging from 98 years to 9975 years and were used for NLTHA, as described in Section 4.2.1. An example set of the selected ground motion records is illustrated in Figure 9.

4.2. Seismic risk

4.2.1. Fragility analysis

In this study, instead of seismically assessing inventories using a taxonomy-based approach to account for the fragility of its assets, and taking advantage of having a complete knowledge of the structural characteristics of all the elements in the case study, an element-based approach implemented by Borzi et al. (2015) was adopted to evaluate the seismic fragility of each bridge in the case study portfolio. Since the focus of this study was not on the derivation of fragility curves for bridges via novel structural modelling and analysis approaches, but on devising prioritization schemes based on risk results, the fragility assessment was carried out adopting the BRITNEY analysis tool and corresponding modelling and limit state definition criteria, as presented in Borzi et al. (2015), with the only innovation being the implementation of AvgSa as intensity measure for the analysis. The tool creates finite element (FE) models for carrying out NLTHA with OpenSees (McKenna, Scott, & Fenves, 2010) and processes the results to characterise the structural response of each bridge in its original, as-built condition (i.e. no ageing effects are considered).

The model elements are either frame elements, elastic for the deck and BeamWithHinges (Scott & Fenves, 2006) for the pier segments and the transverse beams, respectively, or zeroLength elements for deck connections and twoNodeLink elements for bearing devices within super- to sub-structure connections. Nonlinearity is modelled within both frame and zeroLength elements. For this purpose, in the beamWithHinges elements, the cross-section is discretised into fibres. RigidLink elements are also used to model connection dimensions. Uniaxial constitutive models employed for the fibre section of inelastic elements are the Scott-Kent-Park concrete model (Kent & Park, 1971) (Concrete01 in OpenSees) and the bilinear steel model (Steel01 in OpenSees).

For the bearing supports and connections between the deck, piers and abutments, available force-deformation laws in OpenSees (e.g. Elastomeric, FlatSlider, FrictionPendulum) cover the full spectrum of devices, both traditional and modern, typically found in the bridge stocks of Italy. The platform also accounts for simple friction support between two surfaces simply supported, as well as monolithic connections. Furthermore, the tool allows for great flexibility in geometrical definitions to model bridges with complex layouts, such as having a curvature, multiple decks sharing piers, Gerber joints, etc.

In this tool, structural deterioration interactions between elements leading to collapse are not specifically accounted

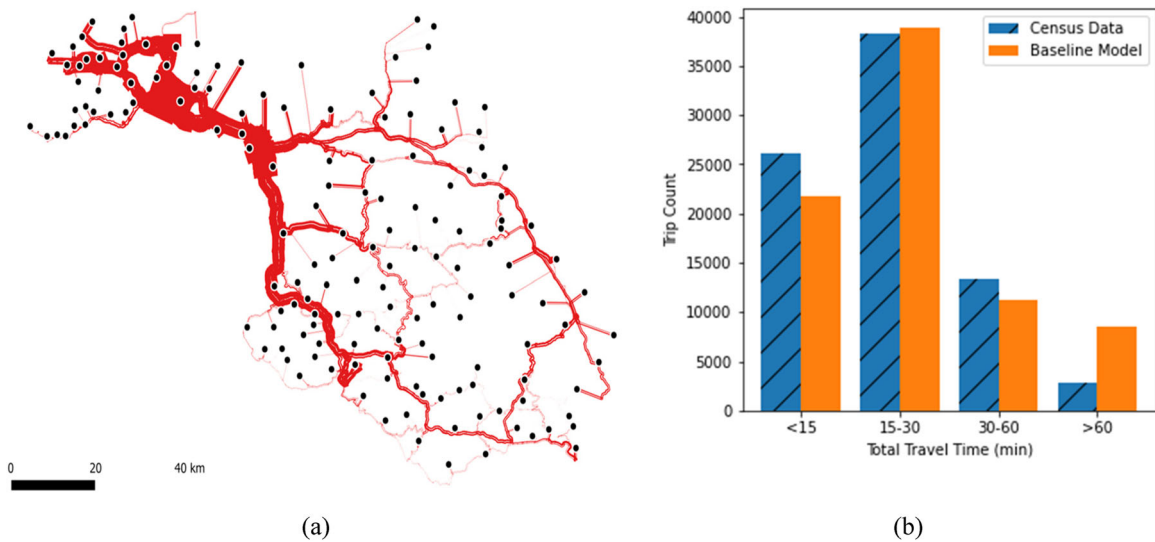


Figure 7. Road network model performance: (a) baseline traffic flows (line thickness is proportional to traffic flow), (b) trip duration comparison of census data with baseline model results.

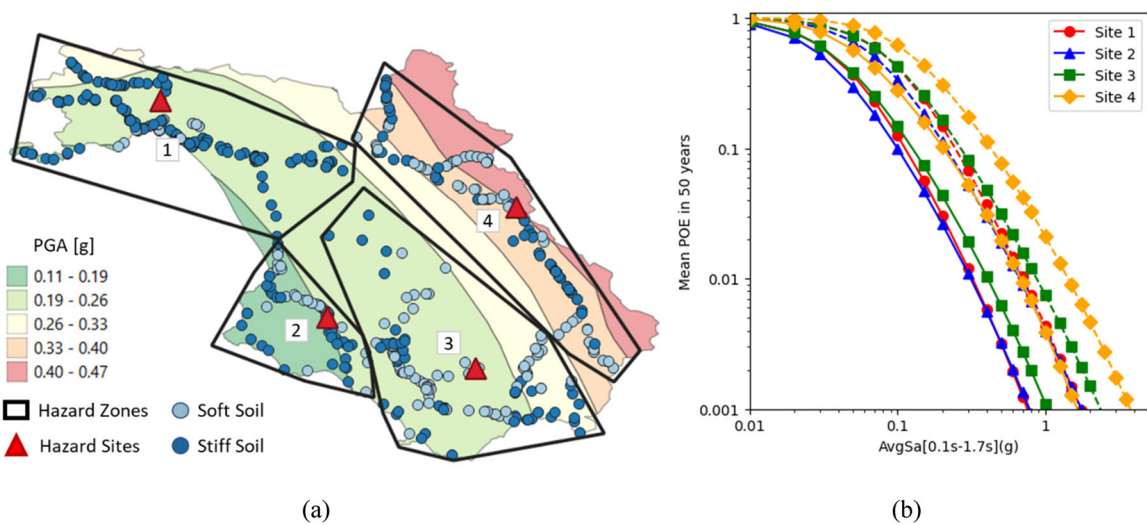


Figure 8. Seismic hazard of the case study region of Salerno: (a) hazard zones and soil sites (PGA values for a return period of 475 years are shown for reference), (b) hazard curves for each hazard zones (dashed lines are soft soil results).

for in the models (i.e. elements will deform beyond the limit response thresholds). However, local demand over capacity ratios were calculated for piers and bearings and, depending on the values of these ratios, damage states were later assigned in the post-processing stage. Piers can fail because either deformation capacity, in terms of chord-rotation, or shear capacity has been exceeded. The shear span L_V was taken equal to the pier height L for single-stem cantilever piers, or in the longitudinal direction, and $L/2$ in the transverse direction of multiple stem piers or piers with monolithic deck connections. The ultimate curvature was determined automatically from a bilinear fit of a section moment-curvature analysis to deal with general cross-section shapes and reinforcement layouts. In terms of shear failure, given the brittle nature of the phenomenon, only a single threshold was defined and associated with the collapse limit state, with the pier shear capacity calculated according to the NTC 2008 equations (M.I.T., 2008).

To account for uncertainty in the capacity thresholds for pier components, these were modelled as lognormal random

variables that were sampled every time an analysis was conducted. The equations used in the definition of the pier thresholds for chord rotation and shear, as well as the logarithmic standard deviation used for the analyses, are presented in Table 3. Further detail on the choice of the different formulations can be found in Borzi et al (2015).

Regarding the bearings, these can suffer from unseating failure, involving the deck and the supporting sub-structure. Bearings can fail due to excessive displacement demand, from simply falling off the deck from the bearing seat, or due to the full loss of support from the pier head. The first condition detects a damage limit state, while the second a collapse limit state. The displacement capacity of the bearings was derived from the pier cap and bearing seat geometry, or directly defined by the user, and was considered as deterministically known.

To account for the bi-directional response under multi-component seismic input, the local D/C ratios, y_i , were taken as the SRSS combination for the piers and bearings,

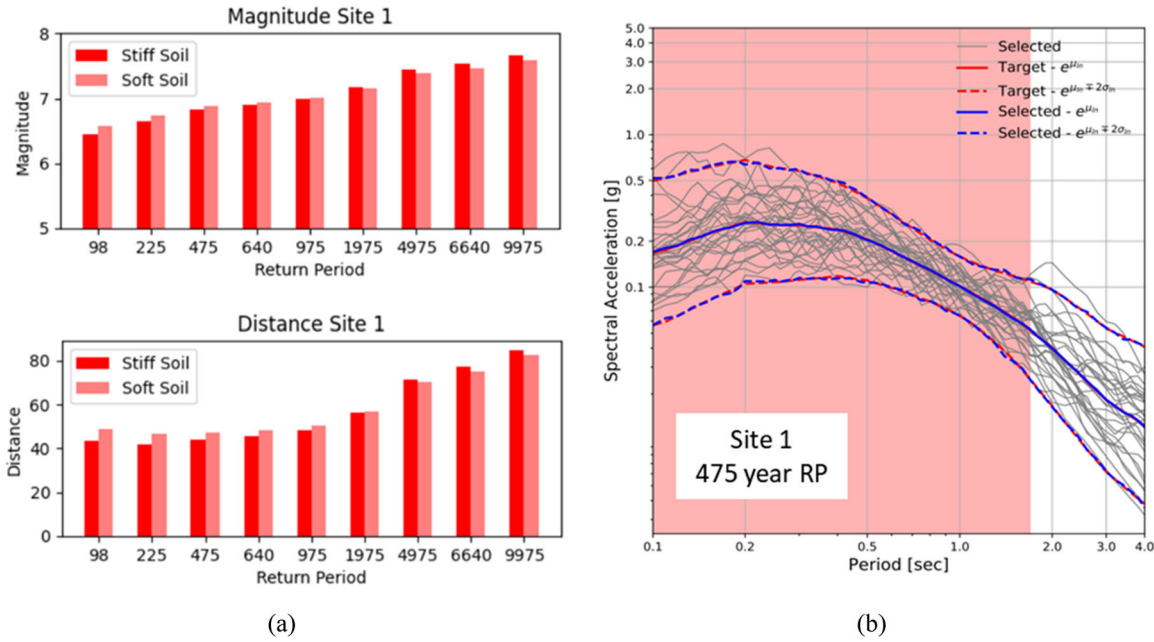


Figure 9. Conditional spectrum record selection: (a) disaggregation results for Site 1, (b) example of record selection for Site 1, 475-year return period, stiff soil.

Table 3. Capacity thresholds for pier segments (h and d_b are the section height and longitudinal bar diameter, respectively) adapted from Borzi et al. (2015).

Limit state	Mechanism	Median	Deviation σ_{ln}
Collapse	Flexure	$\theta_u = \theta_y + (\phi_u - \phi_y)L_p \left(1 - \frac{L_p}{2L_v}\right)$ with: $L_p = 0.1L_v + 0.17h + 0.24 \left(\frac{d_b f_y}{\sqrt{f_c}}\right)$	0.4
	Shear	$V_u = V_c + V_N + V_s$ with: $V_c = k(\mu_{\Delta})0.8A_c\sqrt{f_c}$ $V_s = A_{st}0.9 hf_y$ $V_N = N \frac{0.8h}{2L_v}$	0.25

L_v : Shear length, θ_u : Ultimate rotation, ϕ_u : Ultimate curvature, L_p : Plastic hinge length, V_u : Ultimate shear resistance, V_N : Axial load contribution to shear resistance, V_s : Transverse steel shear resistance, $k(\mu_{\Delta})$: Ductility based reduction factor as per NTC2008, A_c : Concrete shear resistance area, N : Axial load, f_c : conc. compression strength, f_y : Steel yield strength, h : Section height, d_b : Bar diameter, V_c : Concrete shear resistance.

respectively. For example, the local ratio for flexural deformation at the collapse limit state was given in terms of the responses and capacities in the longitudinal (L) and transverse (T) directions as follows:

$$y_{i\theta_u} = \sqrt{\left(\frac{\theta_{iL}}{\theta_{uiL}}\right)^2 + \left(\frac{\theta_{iT}}{\theta_{uiT}}\right)^2} \quad (1)$$

Each sample of demand over capacity ratios, was then used to fit a lognormal distribution of performance for each intensity measure level (IML), as shown in Figure 10. These distributions were then used to evaluate the exceedance of specific limit states and fit a lognormal fragility curve for each bridge. The collapse limit state was focused on since it is the limit state directly related to the complete loss of the bridge connectivity, rendering a straightforward evaluation of indirect losses possible. It is worth noting that more damage states reflecting different levels of damage, and partial bridge closure scenarios, could have been included in the analysis, adopting a similar approach to the one employed by Mackie and

Stojadinovic (2006), who linked bridge functionality to lateral and vertical residual capacity after an earthquake. While this would have been possible, it was opted not to include it to avoid the need for further assumptions related to bridge structural scheme-specific closure thresholds or socio-political decisions, that are specific for the context of each assessed region.

In addition, since no objective information was readily available from Italian sources on how additional limit states would impact the interruption of the bridges (i.e. reduced speed, allowable mass, partial lane closure, etc.); it was decided to focus on the collapse limit state, for which a complete interruption can be expected and information on repair times was available. This decision constitutes a limitation of the current study, since the inclusion of additional limit states will alter the loss estimation and may change the loss-based priority ranking that will be defined in the following sections. However, since all assets in the inventory are being evaluated under the same rationale, the results from this study are still valid from a methodological point of view, within the defined scope and assumptions.

Note that this definition of collapse does not necessarily imply a full and physical collapse of the bridge structure, as in Table 1, but rather a code-oriented definition of incipient or near collapse, essentially implying that the bridge is damaged beyond the point where it may be considered usable, hence interrupting the network. The results obtained for the fragility curves of each element in the inventory are shown in Figure 11, where the mean fragility curve is shown for reference. This lognormal mean curve is represented by the average of all the means of the synthetic bridge models, as described in Equation 2, while the overall dispersion is given by the square root of the sum of squares of the intra-bridge dispersion and the inter-bridge dispersion, as follows:

$$\ln \mu_{\ln Y_{tax}} = \frac{1}{N} \sum_{i=1}^N \ln \mu_{\ln Y_i} \quad (2)$$

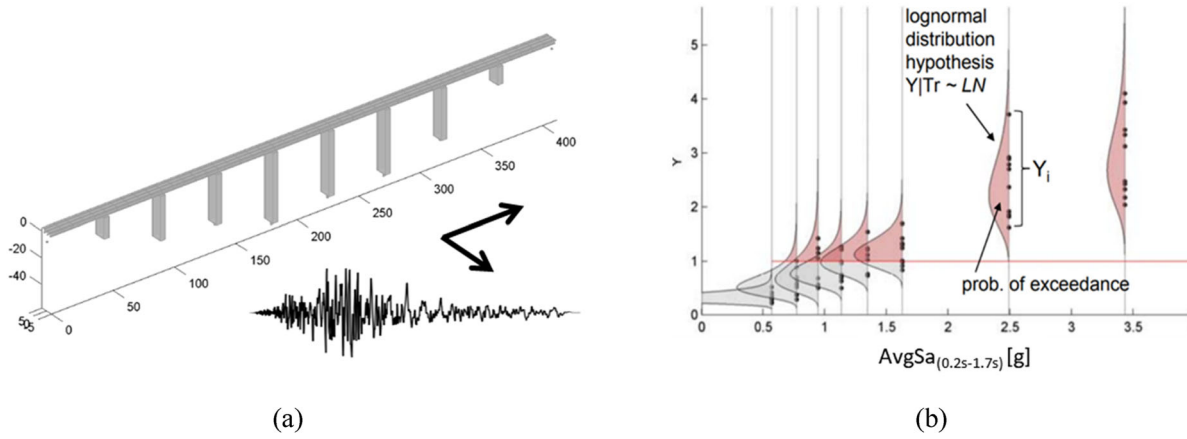


Figure 10. Fragility assessment using BRITNEY: (a) numerical model created with BRITNEY subjected to bi-directional ground motion, (b) determination of probability of exceedance per return period (adapted from Borzi et al., 2015).

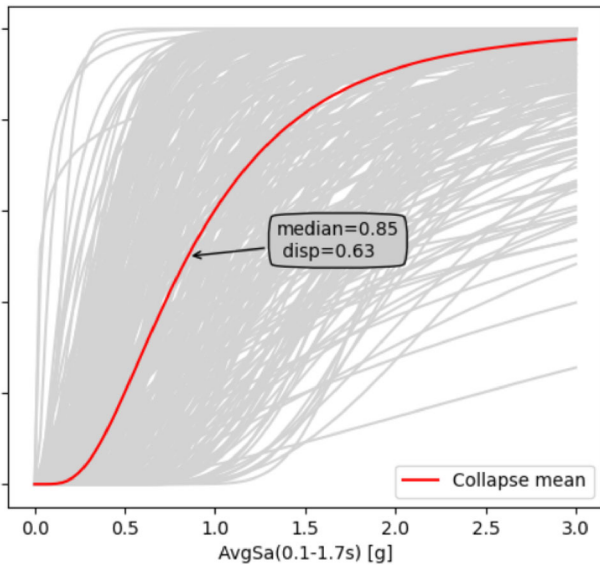


Figure 11. Fragility curves for collapse limit state obtained for the 308 bridges in the database.

$$\beta_{\ln Y_{tax}} = \sqrt{\beta_{\ln Y_{intra}}^2 + \beta_{\ln Y_{inter}}^2} \quad (3)$$

where:

$$\beta_{\ln Y_{intra}} = \frac{1}{N} \sum_{i=1}^N \beta_{\ln Y_i} \quad (4)$$

$$\beta_{\ln Y_{inter}} = \sqrt{\frac{\sum_{i=1}^N (\ln \mu_{\ln Y_i} - \ln \mu_{\ln Y_{tax}})^2}{N}} \quad (5)$$

4.2.2. Direct loss assessment

The calculation of direct losses associated with the collapse limit state was carried out using the basic formulation from the Pacific Earthquake Engineering Research Center's Performance-Based Earthquake Engineering (PEER PBEE) framework (Porter, 2003). A very straightforward implementation of the formulation is possible by including only the collapse limit state, where the product of the annual probability of exceedance of the limit state and the direct

replacement cost will result in the direct collapse-based AAL, as follows:

$$AAL = p(LS_C) \cdot \epsilon L|LS_C = APE_C \cdot \epsilon RC \quad (6)$$

where:

LS_C : Collapse Limit State

$p(LS_C)$: probability of occurrence of LS_C

$\epsilon L|LS_C$: direct economic losses associated to LS_C

APE, LS_C : annual probability of exceedance of LS_C

ϵRC : bridge replacement cost

The annual probability of exceedance (APE) for the limit state was obtained by combining the fragility and hazard curves obtained for each bridge in the case study, evaluating the probability of exceedance in terms of the IML and the respective annual probability of exceeding that IML. The integration over the entire IML range results in the APE for each asset, as shown in Figure 12(a). The replacement cost for each bridge was taken as proportional to the deck area, considering a generic cost per square meter of €930, taken from the mean replacement cost per area obtained by Perdomo et al. (Perdomo, Abarca, & Monteiro, 2020) for a similar Italian bridge inventory. The results for direct collapse-based AAL are shown in Figure 12(b), where it can be observed that higher values of loss are concentrated in the areas with higher seismic hazard.

4.2.3. Indirect loss assessment

Indirect losses for the bridges were considered here as the economic cost that the road network users incur from delays and detours caused by the absence of the connection that the bridge provides between network links. While bridges have been frequently identified as one of the vulnerable components when performing risk assessment of infrastructure networks (Shinozuka, Murachi, Dong, Zhou, & Orlikowski, 2003), their indirect loss component remains a less explored challenge for researchers and practitioners. The reason for this neglect comes in part because of the technical challenge that the calculation represents, but also because the burden of these indirect losses is shared by all the users of the network over a long period of time, making its calculation less feasible and attractive from the point of

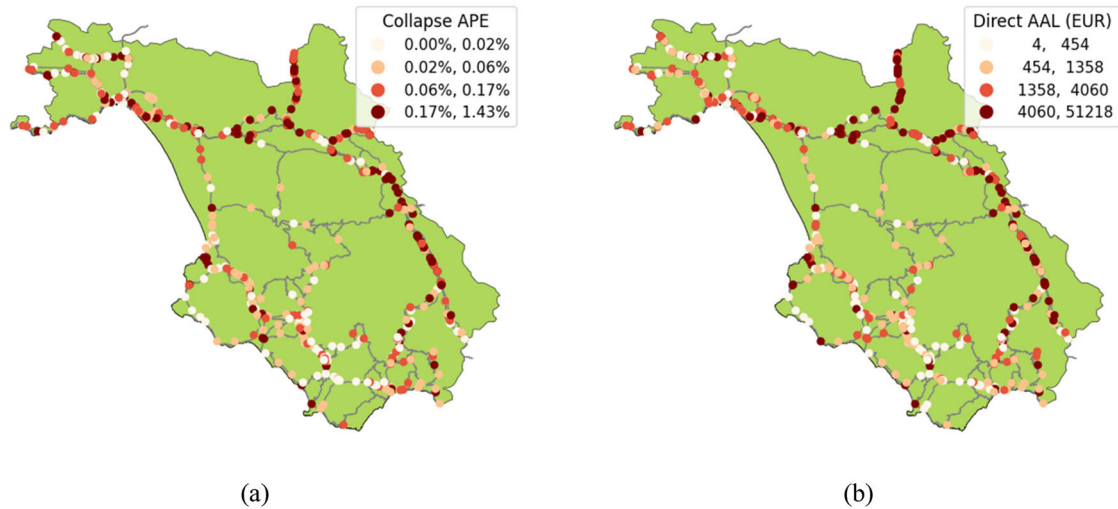


Figure 12. Results for direct loss assessment on the case study inventory: (a) annual probability of exceeding collapse limit state, (b) direct collapse-based average annual losses in Euros.

view of governments and management institutions, who are mostly responsible for coping with the direct losses alone. These issues are common for disaster management of public infrastructure and have been underlined as a worldwide challenge recently in the United Nations Office for Disaster Risk Reduction's Report on Infrastructure and Disaster (United Nations Office for Disaster Risk Reduction, 2015).

In general, the same underlying concept and formulation presented previously to calculate direct losses can be used to determine the corresponding indirect ones; however, the difficulty lies in determining the indirect replacement cost associated to the collapse of the bridge. To determine the indirect replacement cost in this study, the previously described road network model, used to determine the baseline conditions of the network when all bridges are operational, was explored. Two main metrics were obtained from the model: the vehicle hours travelled (VHT), and the vehicle distance travelled (VDT), corresponding to the total amount of time and distance, respectively, that all the users in private cars travelling for work and study purposes in the network experience daily. Both metrics were then combined with median costs for automobile fuel efficiency, fuel prices and hourly salary rates appropriate for the Salerno province (ISTAT, 2020). This allowed the calculation of a baseline daily cost (BDC) of operation of the road network in its current configuration, as shown in Figure 13(a). It is important to note that this baseline cost represents a lower bound, since it does not include trips from freight of heavy transportation vehicles, as discussed in Section 3.2.

Subsequently, the road network was modified by assuming the collapse of each bridge in the network, removing the associated link in the model and rerunning the daily operation cost with the modified network configuration to determine a Modified Daily Cost (MDC) associated with the collapse of each bridge, as shown in Figure 13(b). The total indirect cost of each bridge was then calculated as the difference between the BDC and the MDC multiplied by the repair time in days assumed for each bridge. The computation of the repair time to use for each calculation

represented another challenge. In general, the repair time of bridges varies widely from one case to another, driven mainly by economic and political decisions specific to each case.

For example, following the collapse of the Annone bridge in 2016 (Table 1), it took 33 months to reopen, while the much larger Viadotto Polcevera (Morandi) bridge that collapsed in 2018 took 24 months to reopen, mainly driven by the widespread media coverage of the collapse and relative importance of both bridges to their respective communities. Previous research on this matter relied on repair time models where a probabilistic time is described by some function specific to each country or region, mainly defined through expert opinion. Median repair times used in previous research range from 190 days (Shinozuka et al., 2003) to 450 days (Kilanitis & Sextos, 2018). In this study, the data from the 10 recent collapses in Italy shown in Table 1 was used to fit the lognormal distribution shown in Figure 14 and the median value of 710 days was found and used as a deterministic value for all elements in the case study.

The results for indirect replacement cost and indirect AALs are shown in Figure 15, where it can be seen that the indirect losses were concentrated near the coast of Salerno where the traffic is generally higher, even though the seismic hazard in this area was relatively low. This outcome can be seen as indicative that the monetary value that is incurred by the interruption of points of the road network for extended periods of time outweighs the lower seismic hazard for this case. It is important to note that some of the bridges in the case study that were located near the edges of the Salerno region did not produce indirect loss results when applying this methodology since their collapse resulted in no alternative paths, causing the complete disconnection of some of the centroids. This is a limitation of the applied methodology since alternate routes are likely available when considering neighbouring parts of the road network as well as the residential roads that were excluded from the network model. To avoid this issue in future research, it is possible to either extend the network model beyond the limits of the

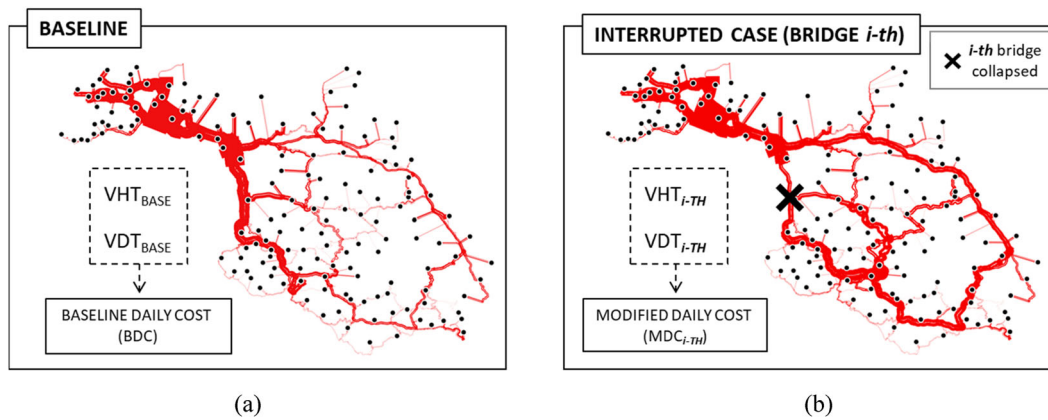


Figure 13. Methodology to determine Indirect Replacement Cost: (a) use of baseline traffic conditions to calculate a daily operational cost, (b) calculation of modified daily operational cost by removing bridge i -th.

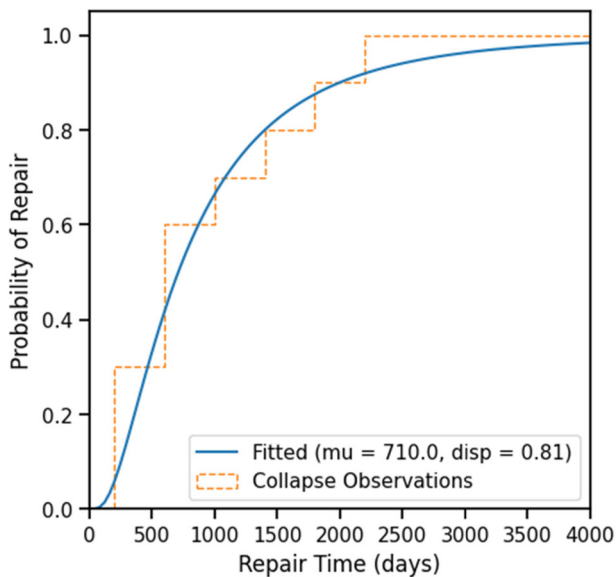


Figure 14. Cumulative histogram and log-normal fit for repair time observations based on recent collapses in Italy.

case study regions or account for the costs of cancelled trips; however, for the purposes of the present study, the analysis will focus herein on the remaining 531 bridges that did produce indirect loss results with the methodology used.

4.3. Total AAL results summary

Once both direct and indirect loss components were determined, the total collapse-based AALs were aggregated for each bridge, resulting in the distribution shown in Figure 16(a). Analysing the overall results, it is seen that the indirect losses represent 78% of the total losses and that the overall losses have a very similar spatial distribution to the one found for the indirect losses alone, which is expected given that these are much greater than the direct loss component. It is important to note that, while the indirect loss component does seem to have a much larger contribution to the overall losses than the direct counterpart, the actual 78% estimate was obtained through the application of the methodology previously presented, considering all its assumptions and limitations. Changes in the repair time of assets, post-disaster travel

demands, accounting for more modes of transportation and the inclusion of the residential road network will undoubtedly have an impact on the results. However, it is outside the scope of this study to provide a definitive estimate of the indirect losses but rather to provide reference values for the purpose of aiding bridge management institutions in decision-making.

It is also worth mentioning that a large portion of the losses are concentrated in very few assets. For example, from the histogram shown in Figure 16(b), only 9 bridges have loss values that are greater than €100,000 but overall, those bridges represent 42% of the total loss for the entire inventory. Such distributions in loss are mostly caused by the extreme values in indirect loss that were calculated for bridges that have a high traffic flow and very long and ineffective alternate routes. This is an important finding since bridge management agencies could use such indications to put measures in place for these assets, such as having fast-deploying temporary replacements ready to reduce the interruption duration and cost.

5. Machine learning prediction of AAL-based ranking

A supervised machine learning model was evaluated using the case-study AAL results presented in Section 4 to assess the feasibility of predicting losses based on limited data, and to gain insights on the effect and relative importance of simple bridge parameters on the prioritisation, defined by sorting bridges based on their individual AAL results. For this case study, the use of the machine learning modelling process was not intended to create a model to be used on bridges outside of the current case study, but rather to take advantage of its capabilities to infer relationships between independent features (i.e. simple bridge parameters and reference hazard values in this case) and their impact on target values of interest (AAL estimates). It is envisaged that these insights could be possibly used in the future to guide improvement proposals on available prioritisation schemes and guidelines.

5.1. Model and database characteristics

A random forest regression model was chosen given its recently demonstrated good performance when compared to

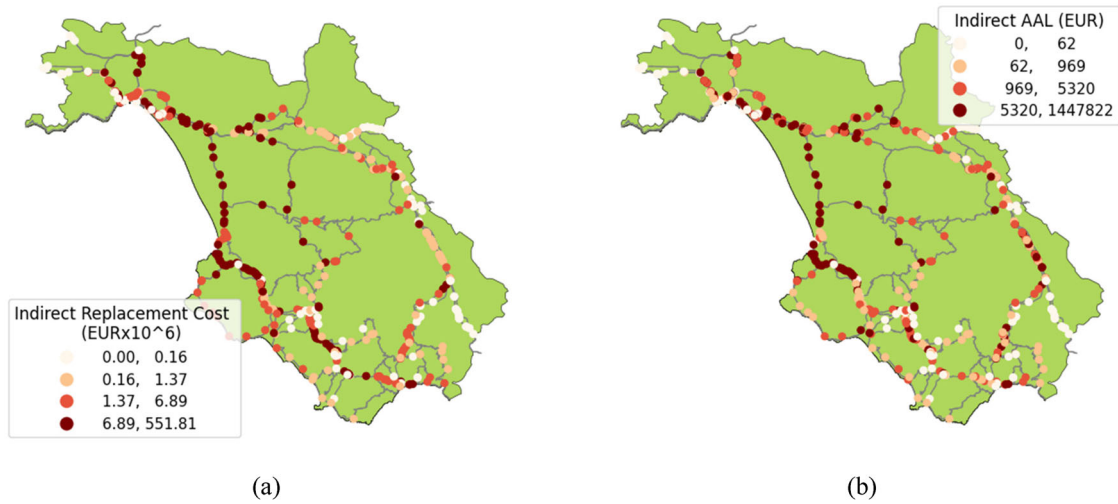


Figure 15. Indirect loss results: (a) indirect replacement cost, (b) results for indirect average annual losses.

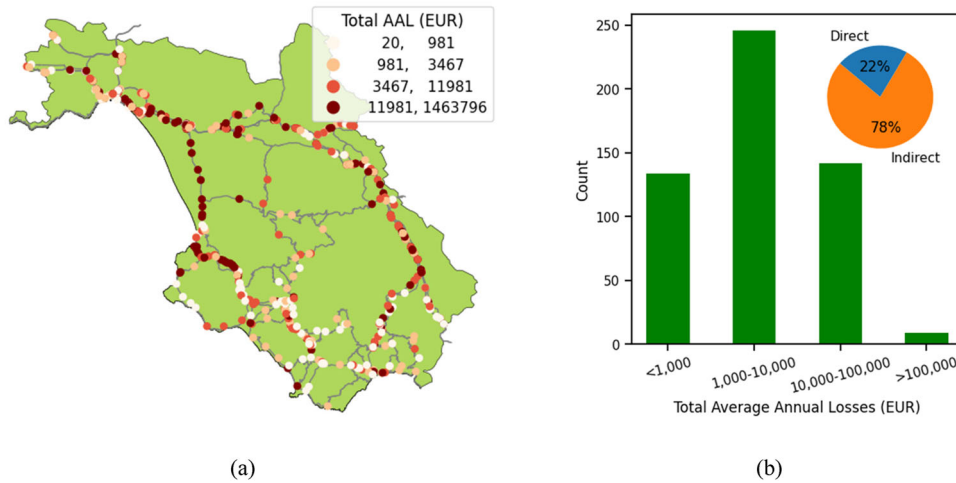


Figure 16. Total average annual loss results: (a) total AAL results for case study inventory, (b) histogram of total AAL results.

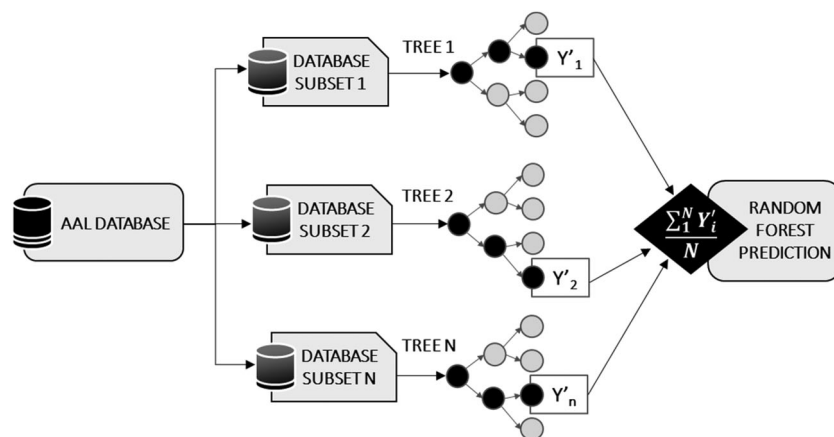


Figure 17. Schematic representation of random forest algorithm prediction methodology.

other machine learning algorithms for similar applications (Mangalathu, Hwang, Choi, & Jeon, 2019), and the ability of this algorithm to evaluate the relative importance of each independent variable. This type of algorithm uses a collection of decision trees built with bootstrapped subsets of the main database, as depicted graphically in

Figure 17. Each tree is fitted to provide predictions based on its sub-sample and all predictions provided by each tree are later averaged to improve the predictive accuracy and control overfitting. The relative importance of each independent variable is calculated by measuring their efficiency in decreasing the prediction uncertainty after each

split of the branches in the tree, averaged over all trees in the forest.

This type of model, as with most supervised machine learning models, uses a labelled dataset that has both its independent variables (inputs) as well as its outcomes, and progressively calibrates its own numerical properties to produce an inferred function that makes predictions about the output values. In order to calibrate the model and evaluate its performance on external data, the dataset is split into a training set, used to fit the model properties, and a testing set used to appraise the fitted properties. The primary model settings were calibrated by running multiple parameter options. The values shown in Table 4 were chosen based on their improved prediction performance evaluated on the testing data set.

A database was assembled using the AAL results for each bridge in the case study to train the random forest model. For this purpose, the AAL representing the dependent variable (target) and a vector of independent variables (or features) was retrieved for each bridge structure. A set of six features were used for each bridge: maximum span length, maximum pier height, daily traffic flow, seismic intensity measure level for a return period of 475 years, number of spans and total replacement cost. Given that all these variables that will be processed by the algorithm have different units and orders of magnitude, each was modified using a minimum-maximum scaling process that transforms the data of each feature by scaling the values within the 0 and 1 range. The resulting database consists of 531 data rows, one for each bridge for which indirect loss results were available, as discussed in Section 4.2.3. It is important to note that the database created is relatively small for a regression problem,

therefore the reader is encouraged to keep in mind that the model performance will be affected by this size limitation.

5.2. Model performance and insights

The evaluation of the regression model on the training and testing sets is presented in Figure 18, along with the relative feature importance, and a set of useful regression performance metrics is presented in Table 5. In general, the model does not have an ideal prediction performance, which is to be expected given the small amount of data points and features used to attempt to predict a complex value such as AAL, which depends on multiple variables that cannot be included in this type of model in a straightforward manner.

In addition, in global terms, when considering the total annual losses aggregated for the entire inventory, the model exhibits a good performance, predicting a value that is 96% of the actual calculated value, however, on the individual asset side, the model tends to overpredict the loss values for most of the elements in the case study, as seen in Figure 19. The underprediction in the global results contrasts with the overprediction on the individual side, however, this is explained by the fact that the expected losses for the entire inventory are governed by outlier assets that exhibit very high values of AAL. When calculated, these AAL values are not accurately predicted by the model since they are represented in the database by very few points, challenging the training of the model in this extreme range.

Overall, in terms of model performance, daily traffic flow has the highest relative importance over all the evaluated features, which is a consequence of the fact that the indirect losses represent the majority of the losses calculated and are directly related to the daily traffic. Moreover, maximum pier

Table 4. Main parameters selected for the random forest implementation after calibration exercise performed on the testing set.

Parameter	Value
Training/Testing split	90/10
Number of estimators	40
Maximum Tree Depth	8
Maximum Features	$\sqrt{\text{features}}$
Minimum Leaf Samples	1
Minimum Split Samples	5

Table 5. Performance metrics for the machine learning model on the entire dataset.

Parameter	Value
Root-mean-squared error (RMSE)	€ 52,279.8
Mean absolute error (MAE)	€ 10,888.2
Median absolute error (MedAE)	€ 3,398.4
Coefficient of determination (R ²)	0.542
Total AAL _{pred} / AAL _{calc}	0.962

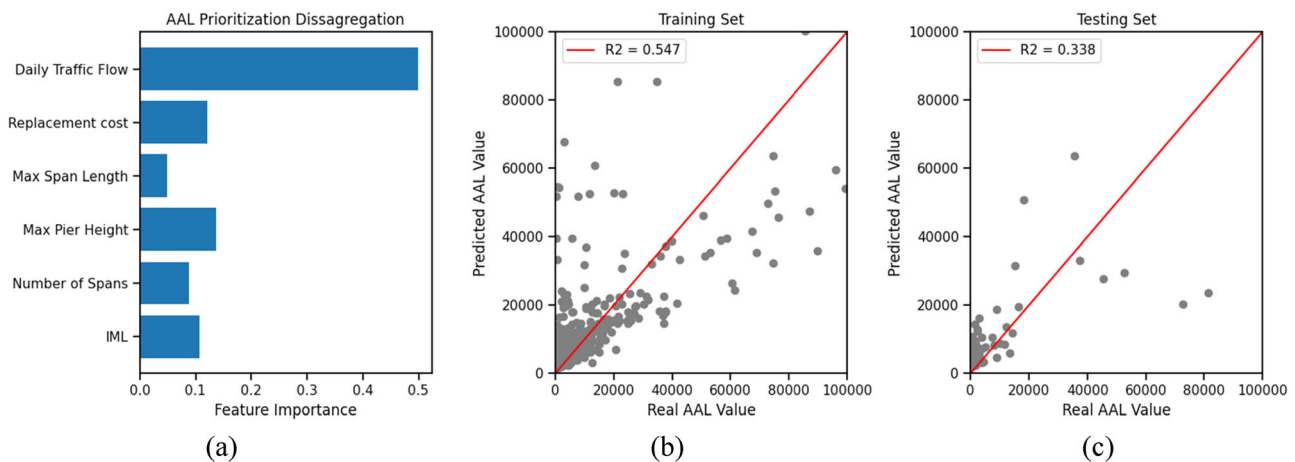


Figure 18. Performance of the machine learning model on the database: (a) feature importance, (b) performance of the model on the training set, (c) performance of the model in the testing set.

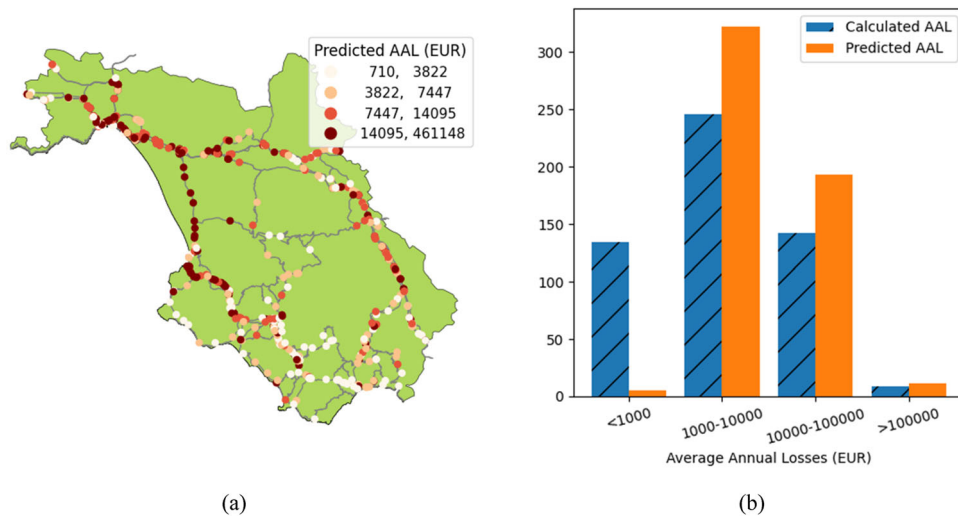


Figure 19. Machine learning model results: (a) predicted AAL results for case study inventory, (b) histogram of calculated and predicted results.

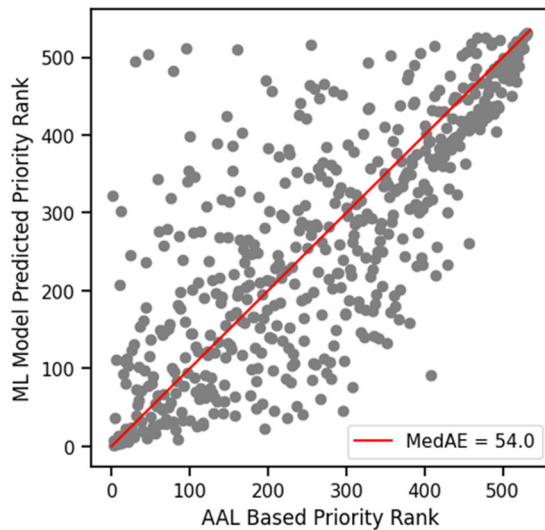


Figure 20. Comparison of prediction prioritisation with benchmark.

height was found to be the second most relevant feature when trying to predict AAL, which is a parameter that is not currently accounted for in the 2020 MIT Guidelines and has been shown to have a correlation with the dynamic properties of bridges in previous studies (Zelaschi et al., 2016). The maximum span length, which has a great impact in the risk classification of the 2020 MIT Guidelines, as will be shown in the following section, has the lowest relative importance as per the machine learning model exercise implemented.

Using the predicted values to determine the priority of assets and comparing it to the one defined by the AAL results actually calculated leads to encouraging results, as shown in Figure 20. The application of the model to only define the relative priority of assets in the portfolio produces a median absolute error of 54 positions, which represent roughly 10% of the total number of assets in the case study.

6. Italian guidelines for bridge portfolio assessment

The 2020 MIT Guidelines propose a multi-level and multi-component approach that classifies bridges in risk categories

through the processing of qualitative metrics, specific to each of the considered hazards: a) structural/foundational, including eventual degradation; b) seismic; and c) flood/landslide. These guidelines have been recently analysed and evaluated by Santarsiero, Masi, Picciano, and Digrisolo (2021), where a thorough summary of the entire classification methodology is presented. In such study, the simple application of the seismic and degradation components of the guidelines to an inventory of 48 bridges concluded that the obtained classification leads to conservative results.

As can be seen in Figure 21, the overall framework of the 2020 MIT Guidelines is organized in six levels of evaluation with increasing degrees of analysis required for each level. Initially, Level 0, concerns the collection of data in terms of location and general geometric and typological characteristics of each bridge from construction documents or inspection reports. Level 1 requires an inspection to be performed on each asset to evaluate the state of degradation of its components in its current state. Level 2 processes the collected information in the previous levels to determine an initial class of attention, of which there are five classes available (low, medium-low, medium-medium-high, high); this level can be seen as a preliminary prioritization scheme from which different assessment actions are required depending on the resulting level of attention class obtained. Level 3 involves a preliminary assessment to be made to bridges with a class of attention of 'medium' or 'medium-high', evaluating in more detail if, based on the typology of the bridge and the defects observed, it merits a more accurate assessment of the individual asset. Level 4, required for bridges with an attention class of 'high' or bridges for which the preliminary assessment considers it necessary, involves a detailed analysis on the asset to evaluate its state as per the current construction codes. Finally, Level 5 is reserved for bridges that are considered of vital importance to the road network, and requires a sophisticated analysis beyond the structural performance, which includes the interaction of the bridge with the network and the social and economical context in which is located.

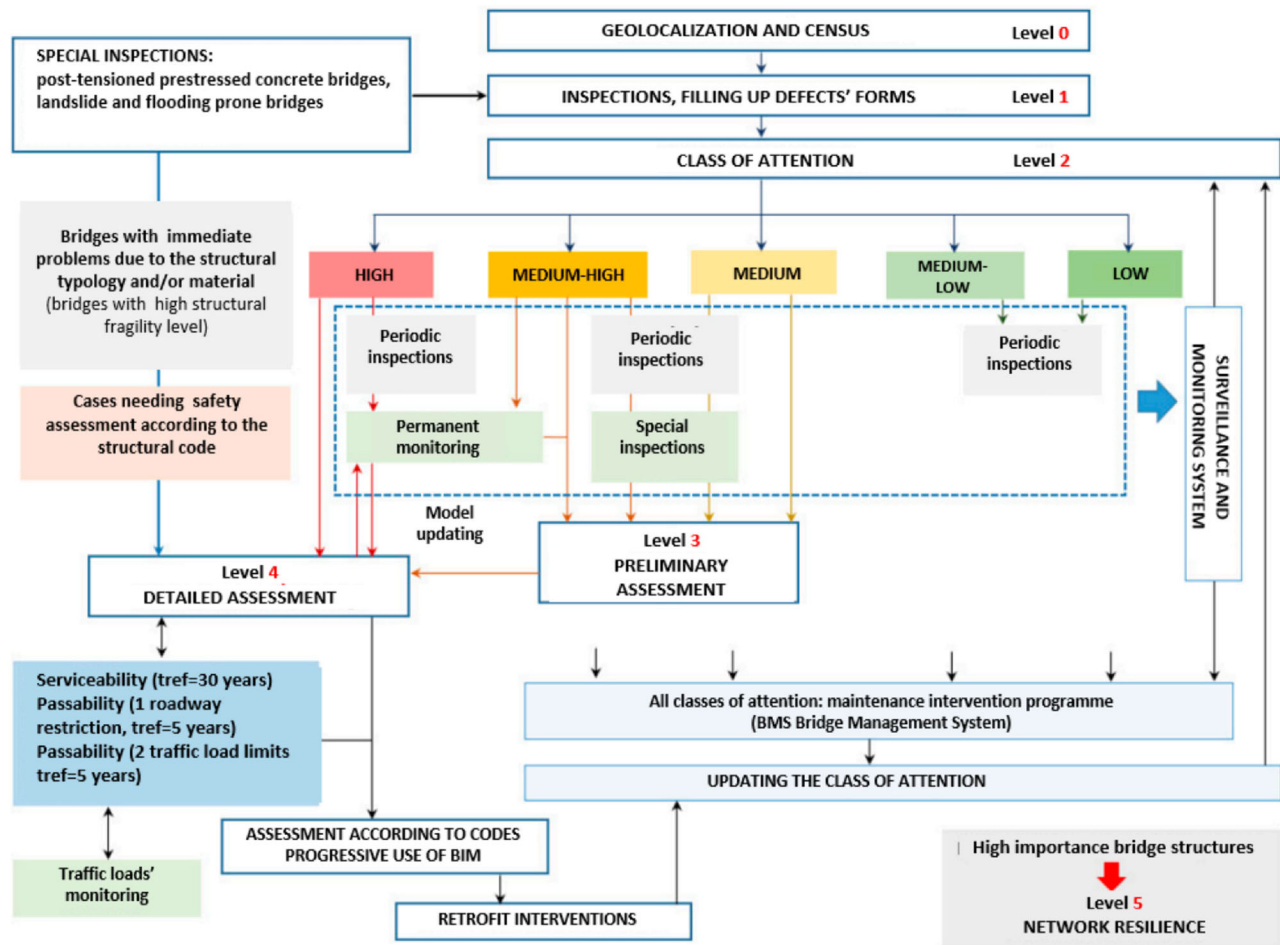


Figure 21. Multi-level framework proposed by the 2020 MIT Guidelines (Santarsiero et al., 2021).

Table 6. 2020 MIT guidelines' seismic risk classification – hazard.

PGA (10% @ 50 years)	Topography		Soil type	
	T1, T2, T3	T4	A, B	C, D, E
0.05–0.10	Low	Medium-Low	+0	+1
0.10–0.15	Medium-Low	Medium	+0	+1
0.15–0.20	Medium	Medium-High	+0	+1
0.20–0.25	Medium-High	High	+0	+1
>0.25	High	High	+0	+1

In the study presented herein, the focus will be only on the Level 2 definition of classes of attention, and only on the treatment of the seismic risk classification of bridges without consideration of structural deterioration, since it is the only component for which the benchmark AAL calculations performed in the previous sections is applicable for comparison. For what concerns seismic risk, as with the other considered risk types, the procedure is divided in the three well-known main components: (a) hazard; (b) exposure; and (c) vulnerability, each of which being assigned one of five possible attention levels that range from low to high. This is done by processing qualitative characteristics of each bridge using a specific set of tabular values, as described in the following paragraphs. After each risk component is processed and a classification is made, all components are convoluted into an overall seismic risk attention class.

In general, the classification of each of the components of risk is determined by a preliminary class, assigned by the

qualitative evaluation of primary parameters that can be further altered by secondary parameters. These may increase or decrease the preliminary classification within the available five classes. The rules for the assignment of the preliminary classes per component are summarised in Tables 6, 7 and 8 for the hazard, exposure and vulnerability facets, respectively. It is also important to note that structural degradation determined from inspections, availability of alternate routes and the consideration of a bridge as strategic, even though qualitative and a little subjective, are also parameters used to alter the classification of a bridge according to these guidelines. For simplification and because this information was not available, these parameters are not included in the tables shown here nor in their application to the case study.

Once each component has been characterised, they are combined to determine an overall seismic risk class, as per the indications shown graphically in Figure 22. As noted by Santarsiero et al. (2021), the overall classification is very much affected by the vulnerability component; for example, if this component is high, then the seismic risk class will be assigned the highest category, almost regardless of the other components.

The methodology foreseen by the guidelines was applied to the case study inventory examined in Section 4, providing the results shown in Figure 23. It can be seen that both the hazard and vulnerability components are mostly classified in

Table 7. 2020 MIT guidelines' seismic risk classification – exposure.

Max span length (m)	Daily traffic (vehicles)			Overpass		
	<10000	10000–25000	>25000	Roads	Rivers	Depressions
<20	Low	Medium-Low	Medium	+1	+0	-1
20–50	Medium-Low	Medium	Medium-High	+1	+0	-1
>50	Medium	Medium-High	High	+1	+0	-1

Table 8. 2020 MIT guidelines' seismic risk classification - vulnerability for RC bridges.

Spans	Max span length (m)		Static system		Seismic design	
	<20 m	>20 m	Hyperstatic	Isostatic	Yes	No
Single	Low	Medium-Low	+0	+2	+0	+1
Multiple	Medium-Low	Medium	+0	+2	+0	+1

the highest possible option, leading to an overall seismic risk class with mostly the high category. This is attributed to the fact that the vulnerability component dominates for simply supported bridges with spans longer than 20 m that have not been seismically designed, which correspond to the predominant characteristics in the case study and to a large portion of the Italian bridge stock.

The obtained seismic category class is compared with the priority AAL rank, defined by sorting the values of AAL in an increasing ranked fashion. The bar plot in the bottom right corner of Figure 23 shows the seismic classification in the vertical axis (with values 1 through 5 representing low to high categories, respectively) while the AAL-based ranking of the 531 bridges in the case study is located in the horizontal axis. The assets with the highest total AAL results are plotted in the first (left) positions. Consequently, if the 2020 MIT Guidelines classification were in complete agreement with the AAL ranking, the bridges with higher risk categories would all be located on the left of the plot and the overall shape of the plot would have a descending trend.

While the classification does seem to group the high and medium-high risk categories mostly in positions that are in agreement with the AAL-based ranking, the fact that there are only two resulting categories and the predominance of the high class creates a problem for the effective implementation of these guidelines as a tool for efficient decision-making and resource prioritisation. As per the 2020 MIT Guidelines, 498 bridges from the 531 in the inventory that were classified into the high category would require the immediate development of detailed structural analysis, implementation of periodic inspections and the installation of monitoring systems. This would clearly require a great number of resources to comply with and be, in some respects, not fulfilling the need of being able to prioritise effectively.

7. Directions for improvement of the prioritisation scheme

Using the insights gained by the application of the seismic risk quantification to the case study in Section 6, along with the influential features found via machine learning techniques in Section 5, a possibly improved methodology to perform bridge prioritisation, based on the same conceptual

framework from the 2020 MIT Guidelines and their observed performance, is outlined and discussed here. This proposed methodology follows the same assessment criteria as the 2020 MIT Guidelines. It thus maintains the ease of application but adapts the evaluation thresholds currently employed to be more in line with the findings of the risk-based prioritization and with the insights gained through the machine learning process employed.

In general, the 2020 MIT Guidelines constitute a robust and well-structured methodology for bridge management. Addressing risk as a convolution of each its three components, as well as the possibility to include multiple hazards, is innovative since it allows for the disaggregation of the risk classification to identify problematic areas and consequently aid in the immediate intervention and retrofitting decision making. The shortcomings that were observed during its implementation are specifically related to the thresholds used to characterise each of its components in a simple and schematic manner, as well as the high relative importance that the vulnerability component has on the overall risk class.

While this conservatism in the vulnerability component was likely a conscious decision made to prioritise bridge safety, it has the downside of classifying a large number of bridges, even those with low associated losses, in the categories of highest priority, which is not in agreement with the findings from a complete quantitative exercise based solely on economic losses, such as the one performed in Section 4. Furthermore, the definition of only five risk classes creates an additional limitation since it can be restrictive when a large, thus more diverse, inventory is considered. For example, as in the results obtained after the classification of the adopted case study, if a large number of assets is classified into a single category, the 2020 MIT Guidelines provide no indication on how they can be further prioritised so that bridge management institutions can efficiently allocate their resources in implementing the monitoring and required explicit analysis actions.

In order to potentially improve the results obtained by the application of the guidelines, the definition of fixed risk classes could be, for instance, changed to an approach based on a point system per component without establishing a limit. The overall seismic risk score would then be composed of the sum of the scores of each component with the available number of points per component being defined as proportional to the findings from the machine learning model, by giving a higher importance to the exposure component and the daily traffic flows, in order to further stress the importance of the indirect losses. In terms of the hazard component, the current thresholds values available in the guidelines are low in comparison to the seismic potential in

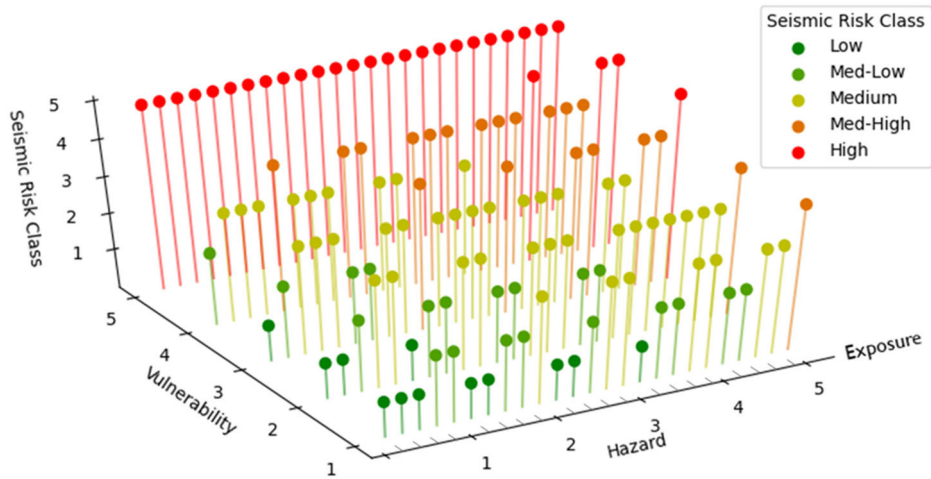


Figure 22. Determination of seismic risk class based on the partial classification of hazard, exposure and vulnerability, adapted from Santarsiero et al. (2021).

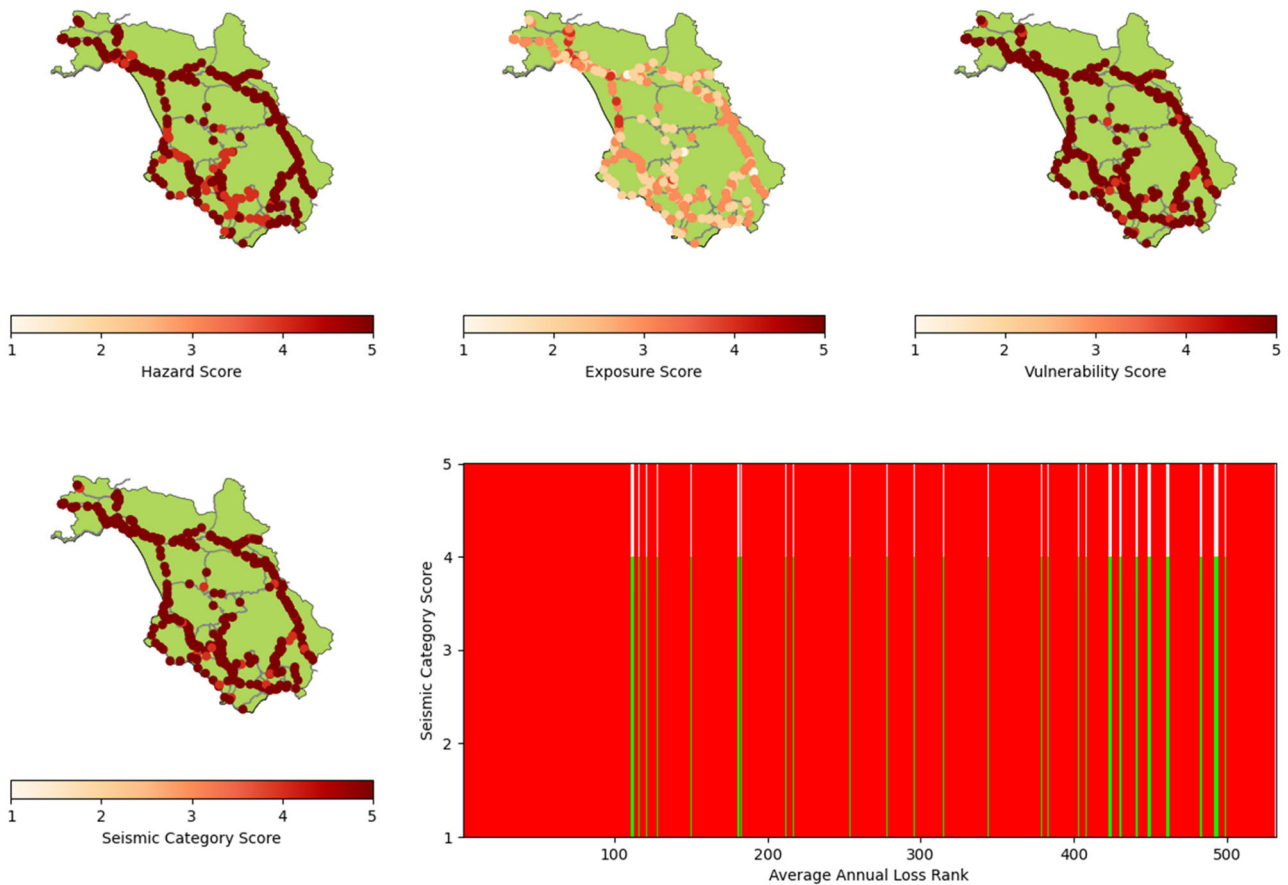


Figure 23. Results for application of 2020 MIT Guidelines to case study inventory.

Table 9. Proposed modified seismic risk classification – hazard.

PGA (10% @ 50 years)	Topography class		Soil type	
	T1, T2, T3	T4	A, B	C, D, E
< 0.10	1	2	+0	+1
0.10–0.20	2	3	+0	+1
0.20–0.30	3	4	+0	+1
0.30–0.40	4	5	+0	+1
> 0.40	5	5	+0	+1

Table 10. Proposed modified seismic risk classification – exposure.

Max span length (m)	Daily traffic			Overpass		
	<4000	4000–10000	>10000	Roads	Rivers	Depressions
<25	1	+3	+5	+1	+0	-1
25–40	2	+3	+5	+1	+0	-1
>40	3	+3	+5	+1	+0	-1

the Italian territory according to the hazard model used (Woessner et al., 2015). Therefore, the values could be

updated as shown in Table 9 to be more applicable to case-study areas of high seismicity according to the hazard model used.

Table 11. Proposed modified seismic risk classification – vulnerability.

Spans	Max span length (m)		Static system		Seismic design		Max pier height (m)	
	<30 m	>30 m	Hyperstatic	Isostatic	Yes	No	<15	>15
<3	1	2	+0	+1	+0	+1	+0	+1
3–10	2	3	+0	+1	+0	+1	+0	+1
>10	3	4	+0	+1	+0	+1	+0	+1

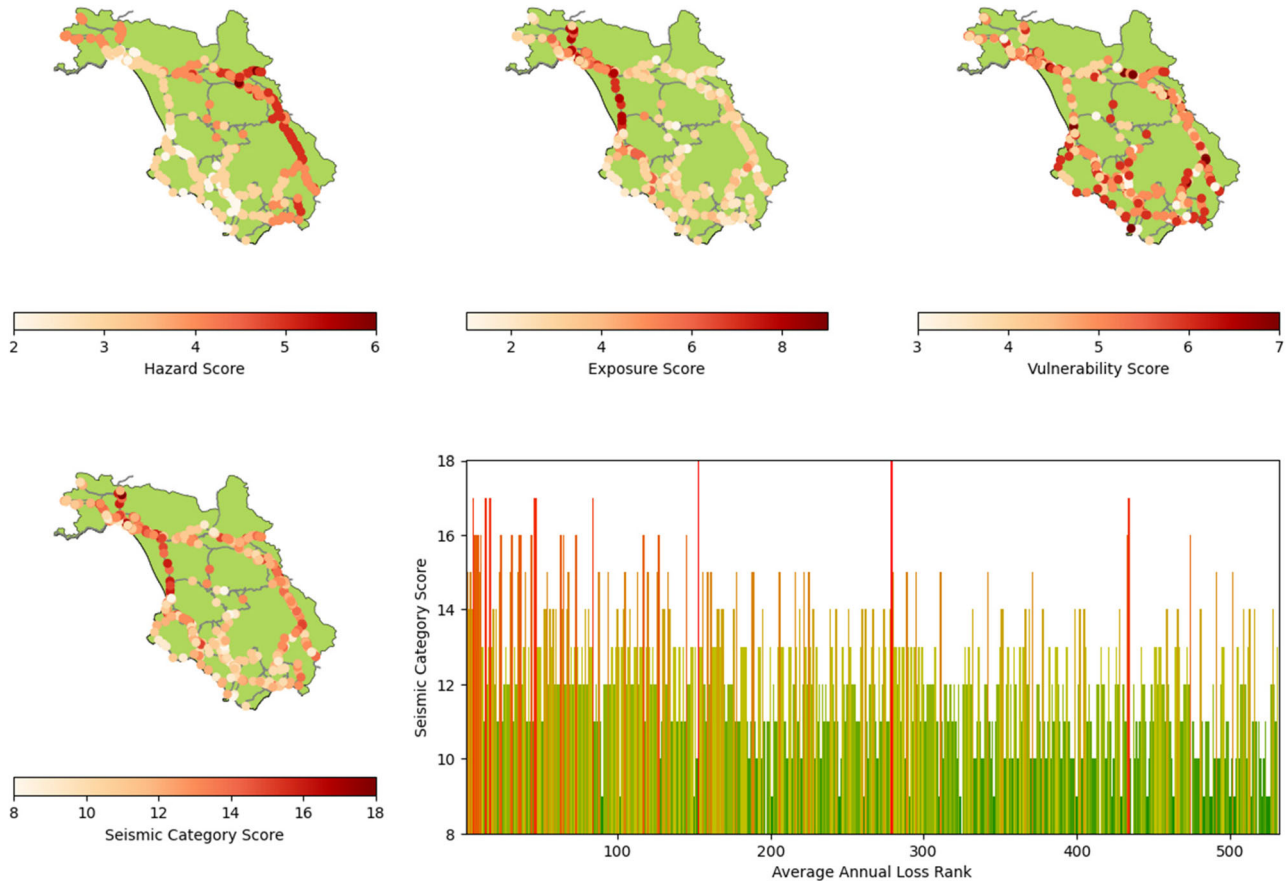


Figure 24. Results for the proposed modified seismic risk classification's prioritization.

Regarding the exposure component, the thresholds for span lengths could be modified to reduce the impact of this parameter on the overall results. Also, traffic flows would be reduced to increase its sensitivity, given that this parameter was observed in Section 6 to be the most influential in the determination of annual losses. Furthermore, to provide more importance to the overall component, the total amount of awardable points would increase as shown in Table 10.

Regarding the vulnerability component, the threshold values for number of spans and maximum span length could be updated as per Table 11, which were calibrated by iterating on different values and observing their effect in the classification performance with respect to the AAL ranking. Furthermore, the maximum pier height would be included as an additional parameter since it was recognised as a relatively important feature during the machine learning experiment, shown in Figure 19(a).

Adopting the described modification proposals, the proposed modified methodology was applied to the same case study, leading to the results shown in Figure 24. It can be observed that there is a higher resolution of results for each of

the components (i.e. no saturation with the high limit), which also translates in a wider range of risk scores for the overall inventory. The spatial distribution of the scores is more in agreement with the loss results and the overall prioritisation performance appears greatly improved with respect to the outcomes of the original guideline's methodology.

It is important to note that, while the definition of the case study and its properties were designed to be considered as representative of a common typology of the bridge network of Italy, the proposed methodology was made by calibrating values from the available database therefore its applicability would be limited to real case databases that would be created following the same methodology as the one used herein, particularly in terms of road network modelling.

8. Conclusions

In this study, a synthetic case study of 617 bridges in the province of Salerno, Italy, was generated by sampling from a database of 308 bridges with complete information and

was used to perform seismic risk assessment considering direct and indirect loss economic losses. The resulting database of collapse-based average annual losses (AAL) was explored using data science techniques to determine the influence of simple bridge parameters on the calculated losses and associated priorities, to ultimately use these insights to evaluate and propose improvements to the recent guidelines on risk classification and management, safety assessment and the monitoring of existing bridges (Consiglio Superiore dei Lavori Pubblici, 2020) – 2020 MIT Guidelines.

The application of the described methodology led to the following conclusions, regarding the prioritisation of bridge assets within a regional portfolio, even with limited information available:

- When data and analysis resources are available to consider both direct and indirect components of loss, AAL can be considered an alternative or complementary metric by which assets within a bridge portfolio can be prioritised in terms of resource allocation, inspection and retrofitting; it was seen here that this metric combines the vulnerability of each bridge, as well as the importance that each element has within the entire road network system in a single decision variable.
- Overall, it is concluded that indirect losses have a higher economic impact on the system when compared to direct losses. Given the complexity in their nature, the order of magnitude of this difference depends heavily on the assumptions made during the assessment process, such as using a single transportation mode, median repair times and excluding the residential road system; however, the large difference observed herein is expected to increase when considering all transportation modes.
- When evaluating the influence of commonly available variables in the results of total AAL, it was seen that daily traffic flow, which is related to the exposure component, seems to have the higher relative importance, in comparison to other bridge structure-specific metrics. This result appears reasonable, given the high contribution of the indirect component of loss to the overall results.
- When evaluating the 2020 MIT Guidelines that have recently been published in Italy, it was observed that the application of the methodology leads to large portions of the inventory classified to the highest-risk available category, creating a challenge in terms of its usefulness as an efficient way to classify bridge priorities and resource allocation. Different reasons can be cited for this effect, such as the limited availability of possible categories and the high importance placed on the vulnerability component that uses somewhat conservative thresholds for its classification, such as the restrictive 20m maximum span length limit.
- Using the insights gained by the analyses made, possible directions for an improved prioritisation methodology were drawn and discussed based on modifications made to the current 2020 MIT Guidelines. While further

scrutiny and additional case studies are needed, such a modified prioritisation scheme performed better, when compared to a benchmark classification analytically based on AAL.

Acknowledgements

The work presented in this paper has been developed within the framework of the project ‘Dipartimenti di Eccellenza’, funded by the Italian Ministry of Education, University and Research at IUSS Pavia. It has also received support from the INFRA-NAT project, co-funded by European Commission ECHO – Humanitarian Aid and Civil Protection (project reference: 783298 – INFRA-NAT – UCPM-2017-PP-AG).

Disclosure statement

No potential conflict of interest was reported by the author(s).

Funding

Ministero dell’Istruzione, dell’Università e della Ricerca.

ORCID

Andres Abarca  <http://orcid.org/0000-0003-4011-1496>
 Ricardo Monteiro  <http://orcid.org/0000-0002-2505-2996>
 Gerard J. O’Reilly  <http://orcid.org/0000-0001-5497-030X>

References

- Abarca, A., Monteiro, R., O’Reilly, G., Zuccolo, E., & Borzi, B. (2023). Evaluation of intensity measure performance in the regional assessment of reinforced concrete bridge inventories. *Structure and Infrastructure Engineering*, 19(6), 760–778. doi:10.1080/15732479.2021.1979599
- Borzi, B., Ceresa, P., Franchin, P., Noto, F., Calvi, G. M., & Pinto, P. E. (2015). Seismic vulnerability of the Italian roadway bridge stock. *Earthquake Spectra*, 31(4), 2137–2161. doi:10.1193/070413EQS190M
- Bozorgnia, Y., Abrahamson, N. A., Atik, L. A., Ancheta, T. D., Atkinson, G. M., Baker, J. W., ... Youngs, R. (2014). NGA-West2 research project. *Earthquake Spectra*, 30(3), 973–987. doi:10.1193/072113EQS209M
- Bureau of Public Roads. (1964). *Traffic assignment manual*. Washington, DC: U.S. Department of Commerce, Urban Planning Division.
- Calvi, G. M., Moratti, M., O’Reilly, G. J., Scattarreggia, N., Monteiro, R., Malomo, D., ... Pinho, R. (2019). Once upon a time in Italy: The tale of the Morandi bridge. *Structural Engineering International*, 29(2), 198–217. doi:10.1080/10168664.2018.1558033
- Calvi, G., O’Reilly, G., & Andreotti, G. (2021). Towards a practical loss-based design approach and procedure. *Earthquake Engineering & Structural Dynamics*, 50(14), 3741–3753. doi:10.1002/eqe.3530
- Chase, S., Adu-Gyamfi, Y., Aktan, A., & Minaie, E. (2016). *Synthesis of national and international methodologies used for bridge health indices*. McLean, VA: Federal Highway Administration. doi:10.13140/RG.2.1.1558.1683
- Consiglio dei Ministri. (2003). Primi elementi in materia di criteri generali per la classificazione sismica del territorio nazionale e di normative tecniche per le costruzioni in zona sismica. Roma: G.U. n. 105 del 8 maggio 2003 - S.o. n.72.
- Consiglio Superiore dei Lavori Pubblici. (2020). *Linee Guida per la Classificazione e Gestione del Rischio, Valutazione della Sicurezza ed il Monitoraggio dei Ponti Esistenti*. Roma: Ministero delle Infrastrutture e dei Trasporti.
- D’Apuzzo, M., Evangelisti, A., Nicolosi, V., Rasulo, A., Santilli, D., & Zullo, M. (2019). *A Simplified Approach for the Prioritization of*

- Bridge Stock Seismic Retrofitting*. 29th European Safety and Reliability Conference (ESREL) (pp. 3277–3284). Hannover: Research Publishing Services. doi:10.3850/978-981-11-2724-3_0592-cd
- Iatsko, O., & Nowak, A. (2021). Revisited live loads for single-span bridges. *Journal of Bridge Engineering*, 26(1), 04020114. doi:10.1061/(ASCE)BE.1943-5592.0001647
- ISTAT. (2014). Matrici del Pendolarismo. Retrieved from <https://www.istat.it/it/archivio/139381>.
- ISTAT. (2020). Report condizione di vita, reddito e carico fiscale 2019. Retrieved from https://www.istat.it/it/files/2020/12/REPORT-REDDITO-CONDIZIONI-DI-VITA-E-CARICO-FISCALE-2018_2019.pdf.
- Kent, D., & Park, R. (1971). Flexural members with confined concrete. *Journal of the Structural Division*, 97(7), 1969–1990. doi:10.1061/JSDIAG.0002957
- Kilanitis, I., & Sextos, A. (2018). Impact of earthquake-induced bridge damage and time evolving traffic demand on the road network resilience. *Journal of Traffic and Transportation Engineering*, 6(1), 35–48.
- Kohrangi, M., Bazzurro, P., Vamvatsikos, D., & Spillatura, A. (2017). Conditional spectrum-based ground motion record selection using average spectral acceleration. *Earthquake Engineering & Structural Dynamics*, 46(10), 1667–1685. doi:10.1002/eqe.2876
- Lin, T., Haselton, C. B., & Baker, J. W. (2013). Conditional spectrum-based ground motion selection. Part I: Hazard consistency for risk-based assessments. *Earthquake Engineering & Structural Dynamics*, 42(12), 1847–1865. doi:10.1002/eqe.2301
- Mackie, K. R., & Stojadinovic, B. (2006). Post-earthquake functionality of highway overpass bridges. *Earthquake Engineering & Structural Dynamics*, 35(1), 77–93. doi:10.1002/eqe.534
- Mangalathu, S., Hwang, S.-H., Choi, E., & Jeon, J.-S. (2019). Rapid seismic damage evaluation of bridge portfolios using machine learning techniques. *Engineering Structures*, 201, 109785. <https://sciencedirect.com/science/article/pii/S0141029619328068>. doi:10.1016/j.engstruct.2019.109785
- Maratini, R. (2008). (*Strumenti per l'analisi dei sistemi di trasporto alla scala regionale: modelli di simulazione e sistemi informativi*). (PhD Dissertation). Università degli Studi di Trieste, Retrieved from <http://hdl.handle.net/10077/2752>.
- Ministero delle Infrastrutture e dei Trasporti (2020). *Decreto M 578 del 17-12-2020*. Roma: Consiglio Superiore dei Lavori Pubblici.
- M. I. T., M. I. (2008). *NTC 2008 - Norme Tecniche per le Costruzioni (in Italian)*. Rome: Ministero delle Infrastrutture e dei Trasporti.
- Mitradjieva, M., & Lindberg, P. O. (2013). The stiff is moving—Conjugate direction Frank-Wolfe methods with applications to traffic assignment. *Transportation Science*, 47(2), 280–293. Retrieved 9 21, 2021 from <https://pubsonline.informs.org/doi/abs/10.1287/trsc.1120.0409>.
- McKenna, F., Scott, M., & Fenves, G. (2010). Non-linear finite-element analysis software architecture using object composition. *Journal of Computing in Civil Engineering*, 24(1), 95–107. doi:10.1061/(ASCE)CP.1943-5487.0000002
- Mohamed Mansour, D. M., Moustafa, I. M., Khalil, A. H., Mahdi, & H., A. (2019). An assessment model for identifying maintenance priorities strategy for bridges. *Ain Shams Engineering Journal*, 10(4), 695–704. doi:10.1016/j.asej.2019.06.003
- O'Reilly, G. J., & Calvi, G. M. (2019). Conceptual seismic design in performance-based earthquake engineering. *Earthquake Engineering & Structural Dynamics*, 48(4), 389–411. doi:10.1002/eqe.3141
- O'Reilly, G. (2021). Seismic intensity measures for risk assessment of bridges. *Bulletin of Earthquake Engineering*, 19(9), 3671–3699. doi:10.1007/s10518-021-01114-z
- OpenStreetMap contributors (2020). Planet dump. Retrieved from <https://planet.osm.org>: <https://www.openstreetmap.org>.
- Ozsarac, V., Monteiro, R., & Calvi, G. (2021). Probabilistic seismic assessment of reinforced concrete bridges using simulated records. *Structure and Infrastructure Engineering*, 19(4), 554–574. doi:10.1080/15732479.2021.1956551
- Pellegrino, C., Pipinato, A., & Modena, C. (2011). A simplified management procedure for bridge network maintenance. *Structure and Infrastructure Engineering*, 7(5), 341–351. doi:10.1080/15732470802659084
- Perdomo, C., Abarca, A., & Monteiro, R. (2020). Estimation of seismic expected annual losses for multi-span continuous RC bridge portfolios using a component-level approach. *Journal of Earthquake Engineering*, 26(6), 2985–3011. doi:10.1080/13632469.2020.1781710
- Porter, K. A. (2003). An overview of PEER's performance-based earthquake engineering methodology. Ninth International Conference on Applications of Statistics and Probability in Engineering. San Francisco, California.
- Rashidi, M., Samali, B., & Sharafi, P. (2016). A new model for bridge management: Part A: Condition assessment and priority ranking of bridges. *Australian Journal of Civil Engineering*, 14(1), 35–45. doi:10.1080/14488353.2015.1092641
- Santarsiero, G., Masi, A., Picciano, V., & Digrisolo, A. (2021). The Italian guidelines on risk classification and management of bridges: Applications and remarks on large scale risk assessments. *Infrastructures*, 6(8), 111. doi:10.3390/infrastructures6080111
- Shahnazaryan, D., & O'Reilly, G. (2021). Integrating expected loss and collapse risk in performance-based seismic design of structures. *Bulletin of Earthquake Engineering*, 19(2), 987–1025. doi:10.1007/s10518-020-01003-x
- Shepard, R. W., & Johnson, M. B. (2001). California Bridge Health Index: A Diagnostic Tool to Maximize Bridge Longevity, Investment. *TR News*, 215, 6–11.
- Shinozuka, M., Murachi, Y., Dong, X., Zhou, Y., & Orlikowski, M. (2003). Effect of seismic retrofit of bridges in transportation networks. *Earthquake Engineering and Engineering Vibration*, 2(2), 169–179. doi:10.1007/s11803-003-0001-0
- Scott, M., & Fenves, G. (2006). Plastic Hinge Integration Methods for Force-Based Beam–Column Elements. *Journal of Structural Engineering*, 132(2), 244–252. doi:10.1061/(ASCE)0733-9445(2006)132:2(244)
- Silva, V., Crowley, H., Pagani, M., Monelli, D., & Pinho, R. (2014). Development of the OpenQuake engine, the Global Earthquake Model's open-source software for seismic risk assessment. *Natural Hazards*, 72(3), 1409–1427. doi:10.1007/s11069-013-0618-x
- United Nations Office for Disaster Risk Reduction (2015). *Infrastructure and Disaster*. Third U.N. World Conference on Disaster Risk Reduction. Sendai. Retrieved from https://www.preventionweb.net/files/40429_infrastructure.pdf.
- Valenzuela, S., De Solminihac, H., & Echaveguren, T. (2009). Proposal of an Integrated Index for Prioritization of Bridge Maintenance. *Journal of Bridge Engineering*, 15(3), 337–343.
- Woessner, J., Laurentiu, D., Giardini, D., Crowley, H., Cotton, F., Grünthal, G., ... Stucchi, M., The SHARE Consortium (2015). The 2013 European Seismic Hazard Model: Key components and results. *Bulletin of Earthquake Engineering*, 13(12), 3553–3596. doi:10.1007/s10518-015-9795-1
- Zelaschi, C., Monteiro, R., & Pinho, R. (2016). Parametric Characterization of RC Bridges for Seismic Assessment Purposes. *Structures*, 7(7), 14–24. doi:10.1016/j.istruc.2016.04.003
- Zelaschi, C., Monteiro, R., & Pinho, R. (2016). Simplified period estimation of Italian RC bridges for large-scale seismic assessment. In M. Papadarakakis, V. Papadopoulos, G. Stefanou, V. Plevris (Eds.), *ECCOMAS Conference 2016*. Crete, Greece: ECOMAS Procedia. doi:10.7712/100016.2237.16427
- Zilske, M., Neumann, A., & Nagel, K. (2011). OpenStreetMap for traffic simulation. Retrieved, 10(21), 2021. from https://depositonce.ub.uni-berlin.de/bitstream/11303/4976/2/zilske_neumann_nagel.pdf.